MARK RESOURCES INCORPORATED

MRI 389-3

IDENTIFICATION OF MOVING GROUND VEHICLES IN SAR IMAGERY

Final Technical Report

A. W. Rihaczek
S. J. Hershkowitz
T. V. Duong

November 1997 (for Period 24 October 1996 - 30 November 1997)

Prepared under Contract No. N00014-96-C-0453 for Office of Naval Research

Submitted to: Program Officer
Office of Naval Research
Attn: William J. Miceli (ONR 313)
Ballston Tower One
800 North Quincy Street
Arlington VA 22217-5660

3878 Carson Street / Suite 210 / Torrance, California 90503-6707 / (310) 543-4746 / FAX: (310) 543-5053

MARK RESOURCES INCORPORATED

19 February 1998

Errata

Program Officer
Office of Naval Research
Ballston Tower One
800 North Quincy Street
Arlington VA 22217-5660

Attention: William J. Miceli (ONR 313)

AD-A332 596

Reference: Contract N00014-96-C-0453--Final Technical Report, MRI 389-3, "Identification of Moving Ground Vehicles in SAR Imagery," dated 11/97 (DTIC AD No. ADA332596)

Dear Dr. Miceli:

Enclosed is a double-sided page (page numbers 17 and 18) to replace the same numbered page(s) in the copy of the referenced document which was mailed to you on 30 November 1997. This replacement page corrects the illustration for Figure 15 on page 18.

We apologize for any inconvenience, and thank you for your understanding.

Sincerely,

Stephen J. Hershkowitz
Project Manager

SJH:bf

Enclosure: One double-sided page for referenced document--as described above

cc: Naval Research Laboratory (w/one copy of Encl.)
Attn: Code 2627
4555 Overlook Avenue, S.E.
Washington DC 20372

Defense Technical Information Center (w/two copies of Encl.)
8725 John J. Kingman Road, Suite 0944
Fort Belvoir VA 22060-6218

3878 CARSON STREET / SUITE 210 / TORRANCE, CALIFORNIA 90503-6712 / (310) 543-4746 / FAX (310) 543-5053

REPORT DOCUMENTATION PAGE

Form Approved
OMB No. 0704-0188

1. AGENCY USE ONLY (Leave blank)	2. REPORT DATE	3. REPORT TYPE AND DATES COVERED
	November 1997	Final 24 Oct 96 - 30 Nov 97

4. TITLE AND SUBTITLE

Identification of Moving Ground Vehicles in SAR Imagery

5. FUNDING NUMBERS

C: N00014-96-C-0453

6. AUTHOR(S)

A. W. Rihaczek, S. J. Hershkowitz, T. V. Duong

7. PERFORMING ORGANIZATION NAME(S) AND ADDRESS(ES)

MARK Resources, Inc.
3878 Carson Street, Suite 210
Torrance CA 90503

8. PERFORMING ORGANIZATION REPORT NUMBER

MRI 389-3

9. SPONSORING/MONITORING AGENCY NAME(S) AND ADDRESS(ES)

Office of Naval Research
Attn: ONR 313
Ballston Tower One
800 North Quincy Street
Arlington VA 22217-5660

10. SPONSORING/MONITORING AGENCY REPORT NUMBER

11. SUPPLEMENTARY NOTES

12a. DISTRIBUTION/AVAILABILITY STATEMENT

12b. DISTRIBUTION CODE

13. ABSTRACT *(Maximum 200 words)*

The objective of this effort was to process and analyze SAR data on moving ground vehicles to determine how they can be identified. The SAR data were collected at China Lake and are known as the Dragnet/MTE data set. The primary conclusion from this work is that the identification procedures we previously developed for aircraft had to be extensively modified in order to be applicable to moving ground vehicles. The fundamentals are still the same, however, namely that the identification must be based on an analysis of complex imagery, amplitude and phase. The resulting analysis and processing procedures show considerable promise in the identification of moving ground vehicles.

14. SUBJECT TERMS

SAR
Identification
Moving Ground Vehicles

15. NUMBER OF PAGES

79

16. PRICE CODE

17. SECURITY CLASSIFICATION OF REPORT	18. SECURITY CLASSIFICATION OF THIS PAGE	19. SECURITY CLASSIFICATION OF ABSTRACT	20. LIMITATION OF ABSTRACT
UNCLASSIFIED	UNCLASSIFIED	UNCLASSIFIED	SAR

TABLE OF CONTENTS

LIST OF ILLUSTRATIONS

LIST OF ILLUSTRATIONS (CONCLUDED)

1. INTRODUCTION

Everyone is accustomed to identifying objects in photographs by visual inspection, so that it is natural to apply the same procedures in the analysis of SAR imagery. Certainly, roads, rivers, and other terrain features are readily recognized in high-resolution imagery. Thus it is commonly believed that ground vehicles should also be readily identified in SAR imagery, provided the resolution is sufficiently high. Indeed, a huge effort has been going into the identification of stationary ground vehicles in SAR imagery.

This effort has not produced the kind of identification performance needed in military applications, in particular if the vehicles are of similar size and shape. The reason is that the backscattering behavior at radar wavelengths is very different from that at optical wavelengths, with the consequence that vehicle identification in SAR intensity imagery will not give the required performance. The intensity image does not contain sufficient information for reliable vehicle identification. However, a SAR system is coherent, so that the image also has phase, not just intensity. The combination of intensity and phase, or the complex image, does contain information for reliable vehicle identification. On the other hand, as soon as one is required to utilize the complex image, quasi-optical approaches to image interpretation are no longer applicable. It is our conclusion that reliable identification of stationary ground vehicles requires the utilization of the complex image, and because of this, also image analysis methods that are totally different from the conventional methods.

With respect to the identification of moving rather than stationary ground vehicles, everyone's idea appears to be that with the inclusion of a motion compensation that removes the motion of the vehicle, the problem becomes that of identifying a stationary ground vehicle. Since we do not believe that truly stationary ground vehicles can be identified from their intensity images, we believe even less that moving ground vehicles can be identified in similar fashion after the requisite motion compensation. However, at the outset of the program we thought that with the inclusion of a good motion compensation we could identify moving ground vehicles from their complex images, as can be done with moving aircraft. This turned out to be incorrect.

The fact is that some vehicles moving slowly on a smooth road can be motion compensated in such a way that the problem reduces to the identification of a stationary vehicle. On the other hand, depending on the design of a vehicle and whether it is moving on a good road, on a poor road, or off the road, an adequate motion compensation may be virtually impossible. Thus we

had to develop a modified approach. We perform only a rather crude motion compensation that removes the gross motion of the vehicle (and does not introduce spurious effects), and then we search for a necessarily short stretch of the data that provides an image of such a quality that feature measurements and vehicle identification become possible, even though the crossrange resolution may be poor. This approach is necessary even in the benign case of a vehicle moving in weak surrounding clutter, or for data collected with effective clutter suppression. In the more practical case of interfering clutter, the motion compensation is even more difficult. In this report we will restrict our analysis to imagery obtained without clutter cancellation.

The variety of vehicles, the different kinds of motion, and the different environments imply that one cannot use a single processing/analysis procedure to deal with all cases. One must have available a variety of procedures, and before starting the detailed processing and analysis one must examine the image and, based on the characteristics of the image, decide on a particular procedure. As in other complicated applications, the identification system thus must operate adaptively.

2. ANALYSIS OF THE TEL

2.1 The TEL Moving in a Circle (Data Set dra010600a092)

After finding the smeared image of the moving TEL in the SAR scene, we perform a crude motion compensation based on the range motion of the entire vehicle and then also on the Doppler motion of the entire vehicle. This will compensate only for the smooth part of the vehicle motion, leaving any higher-frequency variations in the data. The resulting image is shown in Figure 1. The way in which the image is presented is unconventional in that the local maxima in the intensity image are indicated by dots, the size of which are proportional to the intensity peak. This presentation is more convenient for our purposes. The processing time for this image is 2.1 s, centered near the time of 76 s. This intensity image is actually fairly good for a moving ground vehicle. However, to identify the vehicle among those of similar size and shape would not be possible, in particular not in an automated fashion.

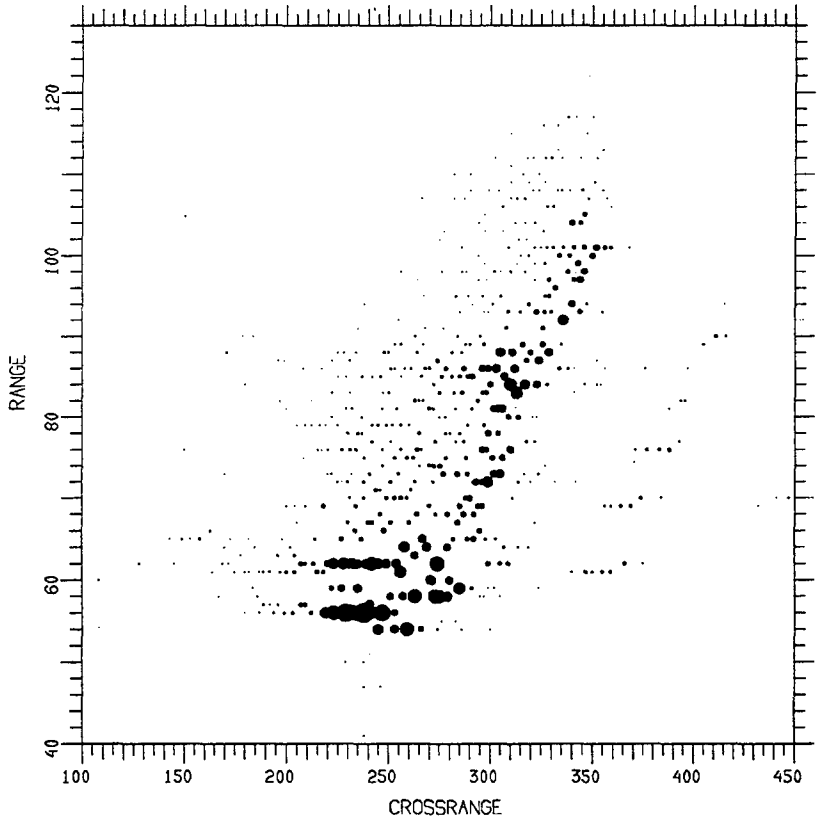

Figure 1. Image of TEL After Crude Motion Compensation.

We must now determine the characteristics of the motion remaining in the image, so as to decide on a specific processing/analysis approach. The goal is to generate an image in which we can determine the locations of scatterers responsible for the stronger image responses. This can be done successfully only with the complex image, but there is no practical way of presenting a complex image. Thus we will show only intensity images, even though the image phase will be used in all analyses.

To determine the characteristics of the residual motion in the image, we would like the vehicle to contain a strong corner reflector. The phase function of the response from this reflector then would show the details of the motion of the corner reflector. We could then select a section of the data over which the motion is one of constant Doppler (or linear phase). Over such a data segment, the corner reflector response then would be properly compressed in crossrange. Actually, since different parts of the vehicle may move differently, we would want to have corner reflectors distributed over the entire vehicle. For each of these corner reflectors we could then presumably find a stretch of the data over which the motion is one of constant Doppler. If we were lucky, these suitable data sections would all overlap in time, so that a single data section would give a good image. If the vehicle motion is so uneven that different parts of the vehicle should be imaged at different times, we may have a problem of relating the Dopplers at the different times, so that the crossrange positions of the responses may be falsified. However, in that case we still could base identification on the range positions, using Doppler merely to resolve responses so that good range measurements become feasible.

Since real vehicles do not contain good corner reflectors, usually not even one, we must perform the search for a good data section on the responses from actual scatterers. Here the problem is that a scatterer is rarely by itself in a given range gate, so that there is interference from other scatterers. This makes it difficult to measure the motion of the scatterer. We will demonstrate how the ideal measurements discussed in the preceding paragraph can be approximated on a real image.

First, we must decide how long a data stretch is needed for imaging. The imaging interval should not be too short, because then Doppler resolution is poor. How much Doppler resolution is needed depends on the size and the orientation of the vehicle. We know approximately the sizes of ground vehicles, and we also know (from experience) that we must subdivide the usable part of the vehicle image into at least about 20 or 30 resolution cells for positive identification. In the case of the image in Figure 1, we can argue as follows. The vehicle extends over about 50 range cells, so that crude

crossrange resolution is satisfactory. If we measure the peak positions of the spread responses that appear as a series of dots in the various range gates, we can estimate that the width of the vehicle is in the order of about 50 crossrange gates. Assuming a practical vehicle width of 3 m (and a good motion compensation), that would imply a crossrange resolution of 6 cm. However, with the vehicle extending over 50 range cells, a crossrange resolution of only 10% should be adequate. Thus we would want to select a data stretch at least about 10% of that used for the image in Figure 1. We also do not want to attempt to achieve too fine a crossrange resolution, because then the motion compensation would likely not be adequate. If the best crossrange resolution we might want to use is 30 cm, we want the data segment to be 10% to 20% of that used for Figure 1.

To find a suitable data segment, we investigate the range gates with the strong or the isolated responses. We start with the range gate containing the strongest response, which is Gate 55.69. The cut through the image in this range gate is shown in Figure 2, the amplitude function on top and the associated phase function at the bottom. If this is the smeared response from a single dominant scatterer, then the transform will give an essentially constant amplitude. In that case the phase function will describe the motion of the scatterer, so that a good data segment can be selected.

The actual transform of the image cut is shown in Figure 3 (the amplitude response has been deweighted). Since the amplitude is strongly modulated, this image cut does not meet our criteria for selecting a good data segment. However, if no better image cut were found, we still could use this one. Provided the phase jumps remain much smaller than half a cycle, the general trend of the phase function will be a good indication of the motion of the dominant scatterer. In this instance, the section centered at the normalized time of 0.2 s would likely be a good choice. However, we must examine other image cuts and choose the best one.

One of the better image cuts is found in Range Gate 57.91, as shown in Figure 4. Its transform is given in Figure 5. We see an amplitude with an acceptable degree of modulation, and a maximum phase deviation of only 0.1 cycle over the marked section. Thus we may choose the time interval between the normalized times of -0.33 and -0.16 s.

As mentioned above, it is desirable that the same time segment also be suitable for other parts of the vehicle, in which case we can expect a good quality image without having to accommodate time sections that vary over the vehicle. In Figure 6 we show the transform of the image cut in Range Gate 92.37, with the selected time section marked. As seen from the figure, the

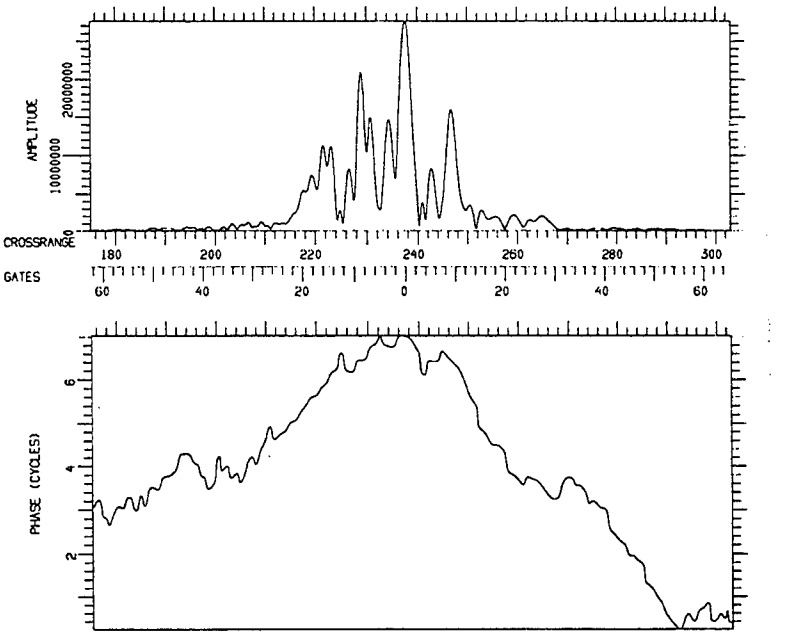

Figure 2. Image Cut in Range Gate 55.69.

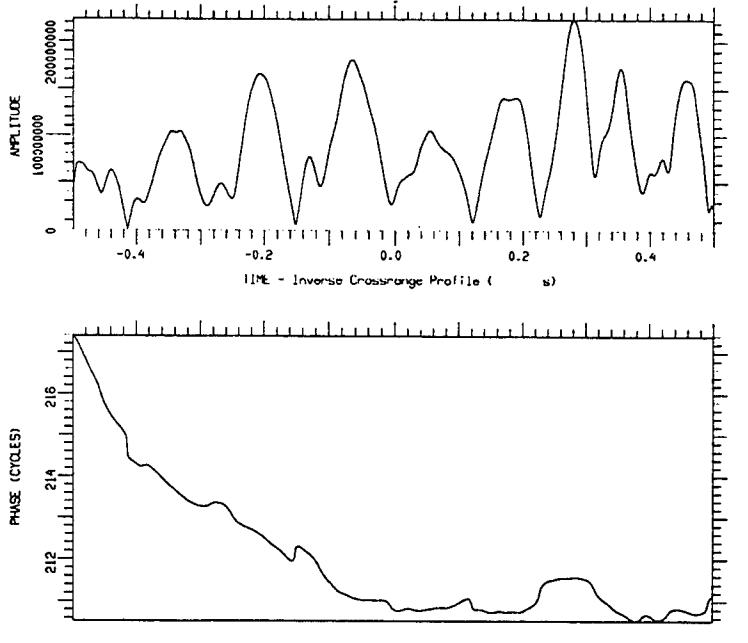

Figure 3. Transform of Image Cut in Figure 2.

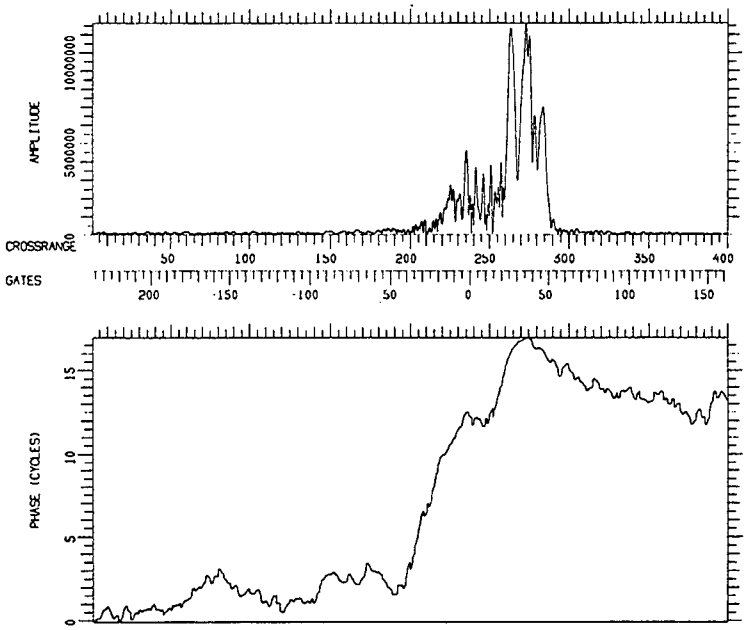

Figure 4. Image Cut in Range Gate 57.91.

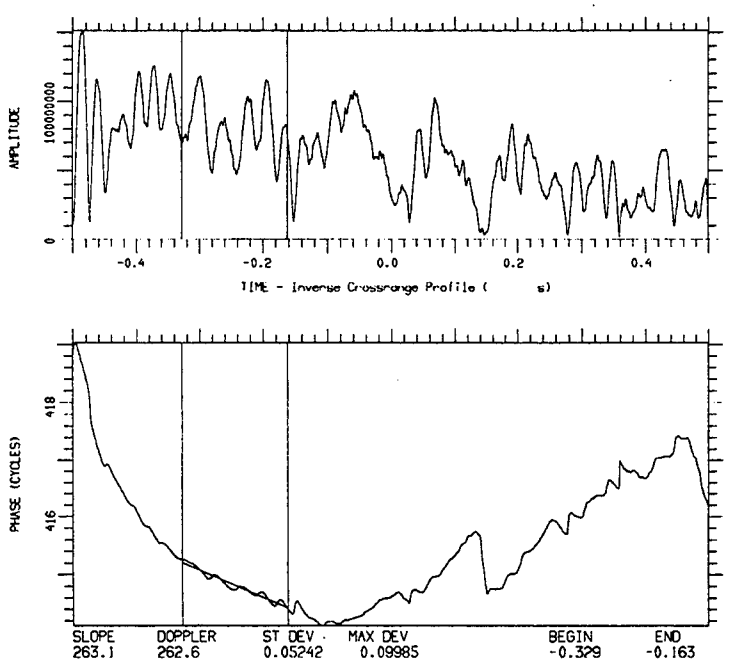

Figure 5. Transform of Image Cut in Figure 4.

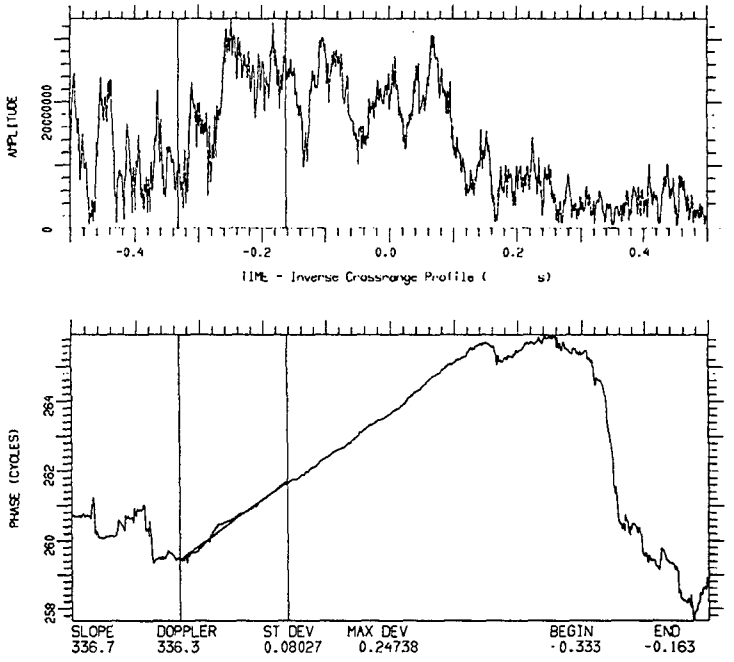

Figure 6. Transform of Image Cut in Range Gate 92.37.

phase is quite linear. Although the printout gives the maximum phase deviation as 0.25 cycles, which would still be acceptable, this maximum deviation occurs at a minimum of the amplitude pattern, and hence is harmless. Thus we have selected an imaging interval that will give a good image. It may be the best interval for this particular image.

The image over the time interval selected above is shown in Figure 7, again in peaks plot form. This image still has so many low level responses that the residual motion is not as constant in Doppler as one might wish. Since vehicle identification will depend primarily on the scatterers near the edges and range resolution is very high, it appears preferable to reduce the imaging time further. In Figure 8 we show the transform of the image cut in the range gate of the strong response near the center of the image, Range Gate 34.03. The amplitude function is sufficiently constant for the phase function to be representative of the scatterer motion. We see a definite kink in the phase function. If we choose only the right half of the time interval, the trend of the phase function is nearly linear. Thus we reduce the imaging interval by another factor of two.

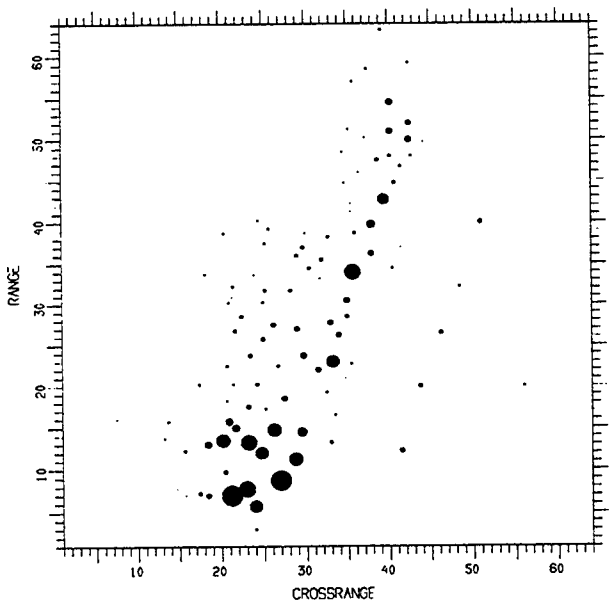

Figure 7. Image Over Time Interval from -0.33 to -0.16 s.

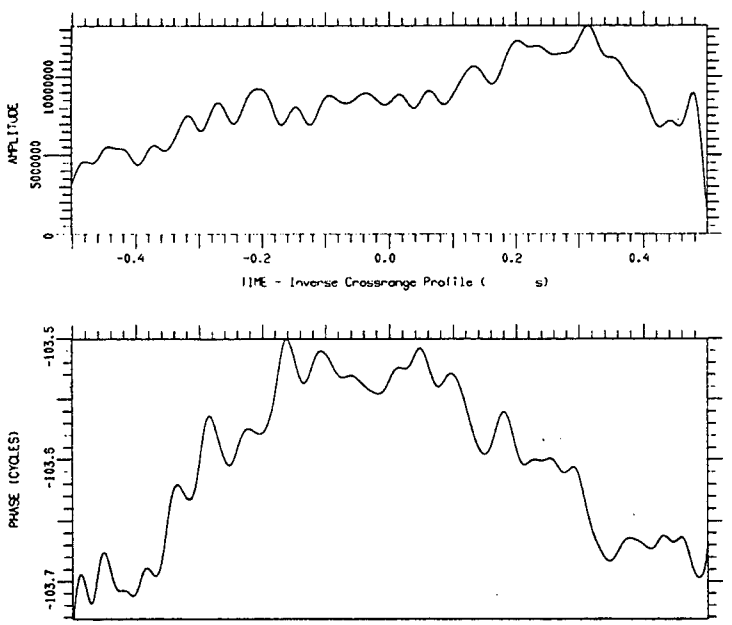

Figure 8. Transform of Image Cut in Range Gate 34.03.

Note that this reduction will help the image quality, but in general will not give an image equivalent to that from a stationary vehicle. The reason is that the individual parts of the vehicle may not move in the same fashion, because the vehicle may be flexible and its individual parts may slowly vibrate in a different manner. In our example, a check of the major responses shows that most move so that their phase functions are linear over the second part of the time segment. The image quality thus is expected to be as high as one can wish under these circumstances.

The new image is shown in Figure 9. Compared with Figure 7, we see a scarcity of dots, also in the range dimension where resolution has not been reduced. This is an indication of high image quality. A ground vehicle has relatively few significant scatterers, so that an abundance of responses indicates motion compensation problems. It is much preferable to have reduced crossrange resolution than a poor motion compensation over the imaging time.

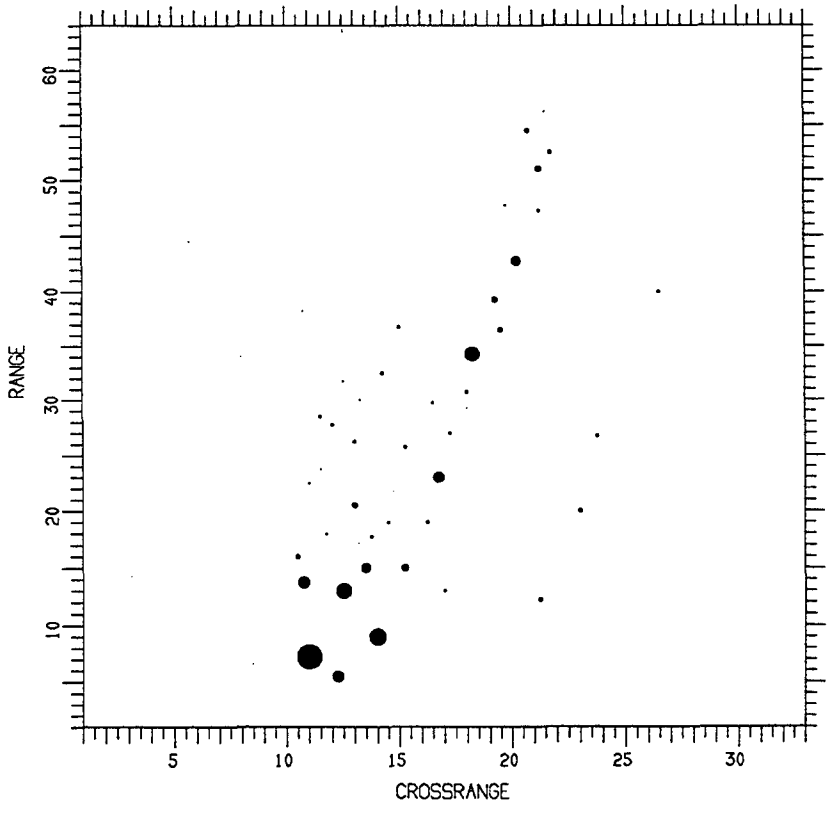

Figure 9. Peaks Plot Image with Reduced Imaging Time.

The complex image corresponding to Figure 9 is now analyzed, so that from the positions of the local intensity maxima indicated by the dots, we derive the positions of the actual scatterers. The corresponding analysis technology is far too complicated to describe in this report, but it is treated extensively in a recent book by the authors [1]. We merely point out that the amplitude and phase functions of each response are analyzed to determine the positions of one or more scatterers contributing to the response. Whereas the peaks in the intensity image often are determined by interference among the scatterers, our analysis yields the true scatterer positions. Also, we might determine the nature of a scatterer from the amplitude and phase functions of its response, depending on the interference conditions.

The primary way of identifying a vehicle from the scatterer positions extracted from the image is to fit these positions to templates of predicted scatterer positions for all candidate vehicles, rotating each template and stretching it in crossrange (because of the unknown crossrange scale factor) until a best fit is obtained. The vehicle with the best fit is then chosen as the one represented by the image. This template match is augmented by other information extracted from responses, to the degree available.

In the case of the TEL, a significant difficulty arose from the fact that the available digitized photographs of the vehicle from various aspects were difficult to use for extracting positional information on the various scatterers. Even the identification of scatterers was sometimes difficult or impossible. Nevertheless, the information about the vehicle was adequate for demonstrating our approach to vehicle identification.

The template match for the scatterer positions extracted from the image in Figure 9 is shown in Figure 10. The measured scatterer positions are marked by crosses, and the positions of the predicted vehicle features by capital letters. For these position matches, the axis scales are in tenths of gates (one gate is the nominal resolution of 1/B in delay and 1/T in Doppler, where B is the bandwidth and T is the coherent dwell). The list of features that were identified by us, mostly near the edges of the vehicle, is given in Figure 10. A question mark means that we did not have a photograph suitable to identify a specific feature observed in the image. Since the differences in the behavior of the individual scatterers are small for this vehicle, and because of the short processing time, the discrepancies between measured and

---

[1] Rihaczek, A. W., and S. J. Hershkowitz, *Radar Resolution and Complex-Image Analysis* (Artech House, 1996).

predicted feature positions are likely caused mostly by measurement errors due to interference, or to the inaccurate extraction of feature positions from photographs. Nevertheless, the match indicated by Figure 10 appears more than adequate for identifying the vehicle even if other vehicles were of a similar size. There is no competing vehicle among the ones contained in the Dragnet database.

To provide a feel for the robustness of the approach, we performed a match for the same vehicle for a somewhat worse time interval, and a longer one than should be used. We selected the time interval from 0.19 to 0.36 s, on the same time scale used in Figure 5. As can be seen from that figure, the phase is still quite linear over this time interval, discounting the large phase variations corresponding to the minima in the amplitude function. On the other hand, the new time interval is not well chosen with regard to Figure 6. At least we cannot be sure, because the break in the phase function at 0.25 s can be due either to a change in the velocity of a single scatterer, or a change in dominance from one scatterer to another. In other words, it is not a safe selection, even though Figure 5 indicates it might be acceptable.

The image over the new time interval is shown in Figure 11. Compared with Figure 9, there are more responses because of the longer imaging interval. This problem is partly remedied by analyzing only the stronger responses. Since the aspect angle has changed between the two imaging times, in principle we might observe a few new scatterers. Thus we tried modifying the database of predicted scatterers somewhat in order to obtain a better positional match.

The positional match for the new image is shown in Figure 12. As is seen from a comparison of the lists of features in Figures 10 and 12, most of the features remained the same. However, with the new image we also have more unidentified "scatterers," probably because of problems with the image. Still, even this lower quality image may suffice for identifying the TEL.

2.2 The TEL on a Straight Smooth Road (Data Set dra011400a084)

The peaks plot image of the TEL moving on a straight and smooth road is shown in Figure 13, after a motion compensation consisting only of the range and Doppler correction for the entire vehicle. The high degree of smearing of the responses in crossrange implies a significant residual motion with nonconstant Doppler. The situation is poor because, due to the small aspect angle, the Doppler caused by the apparent turn motion of the vehicle is much smaller relative to the "vibration" Dopplers than for the TEL moving on a circle. In order to obtain adequate crossrange resolution, the imaging time thus must be chosen so large that the vibrations of the individual parts of

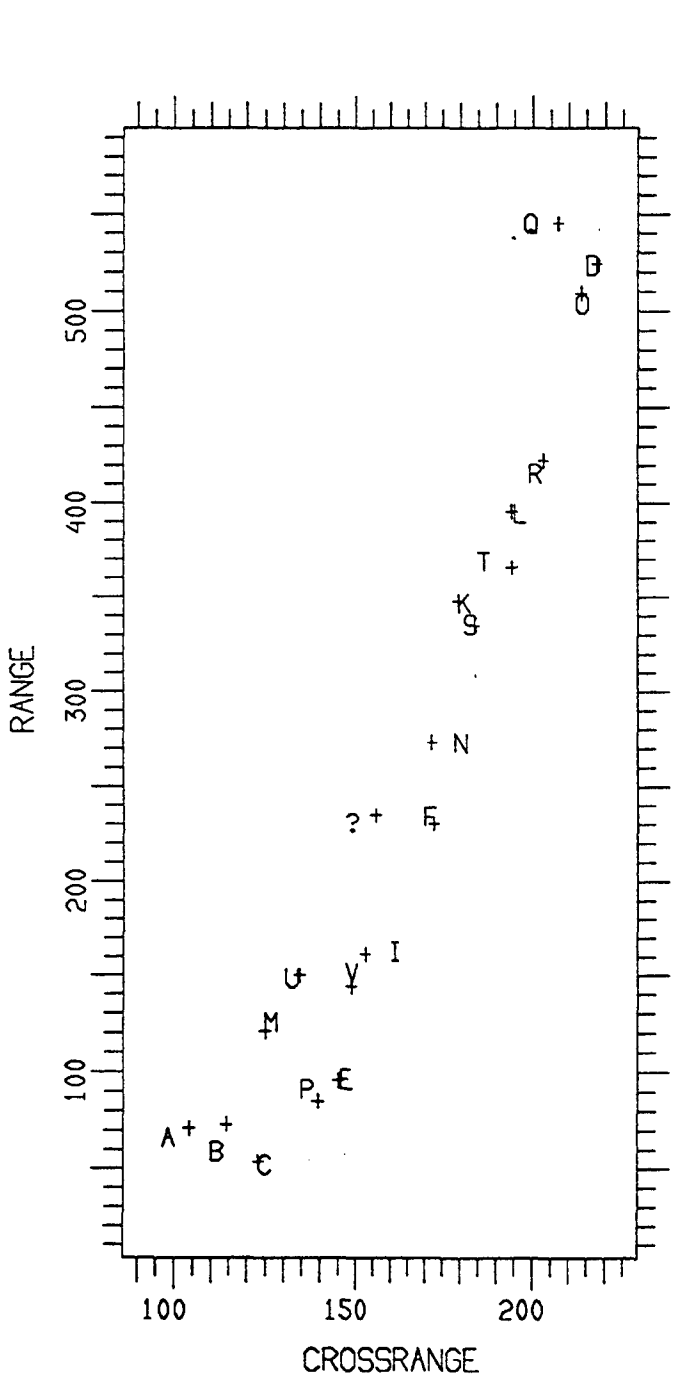

Asp Ang	164.20
Bank Ang	-6.00
Pitch Ang	2.00
C Res	0.47
Roll Shr	0.00
Flex Shr	0.00
Pitch Shr	0.00

A Exhaust Defl LS
B Exhaust Defl Cn
C Exhaust Defl RS
D Door
E Corner Refl
F Fire Exting/Com
I St Comptmnt
K ST Comptmnt
L Brake Block
M Cavity
N Door
O Door Handle
P Cavity
? Unidentified
Q Cab Corner Post
R Brake Block
S Corner
T Hole
U End Fin
V Support

Figure 10. Positional Match for Image in Figure 9.

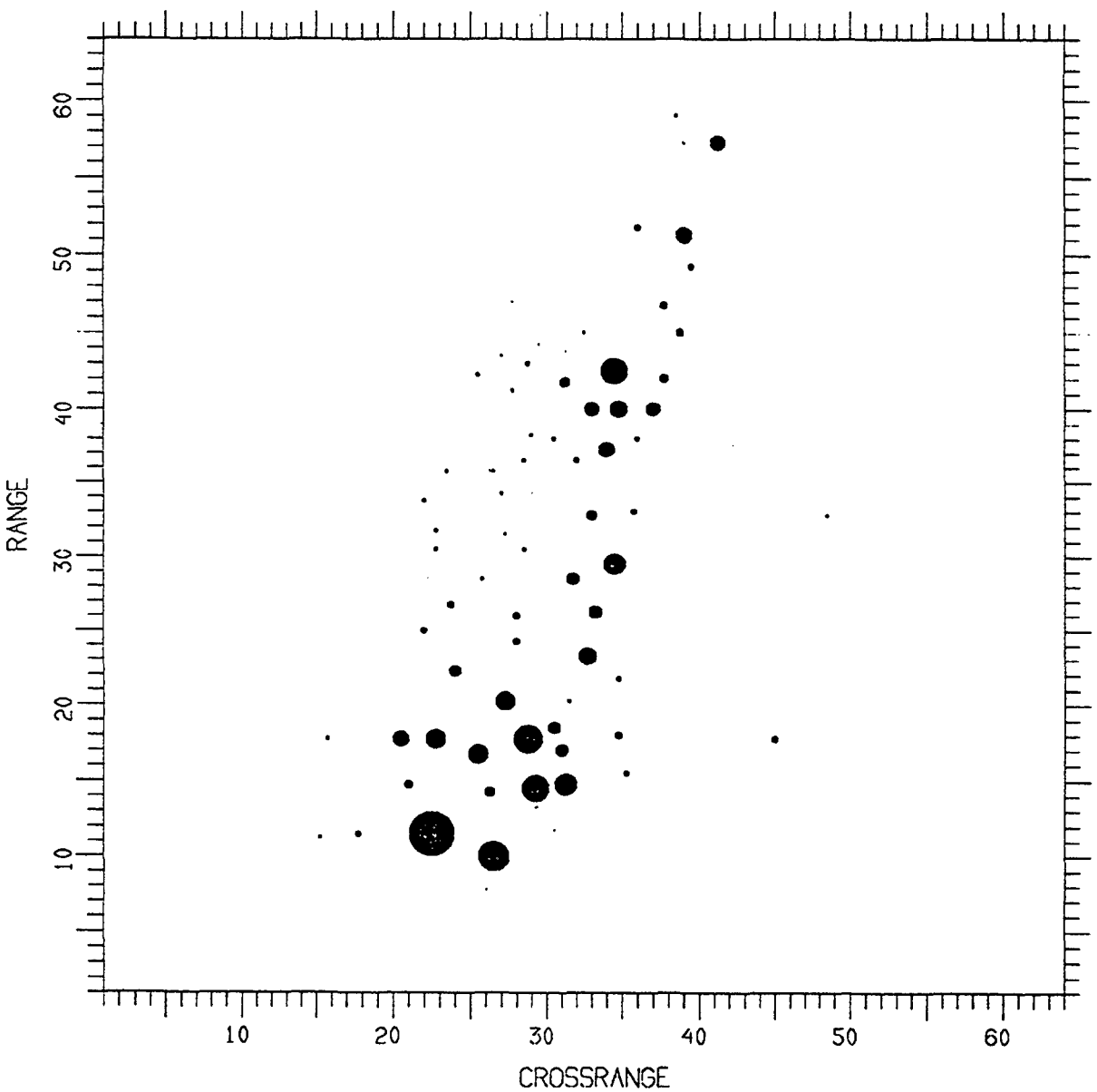

Figure 11. Image Over Time Interval from 0.19 to 0.36 s.

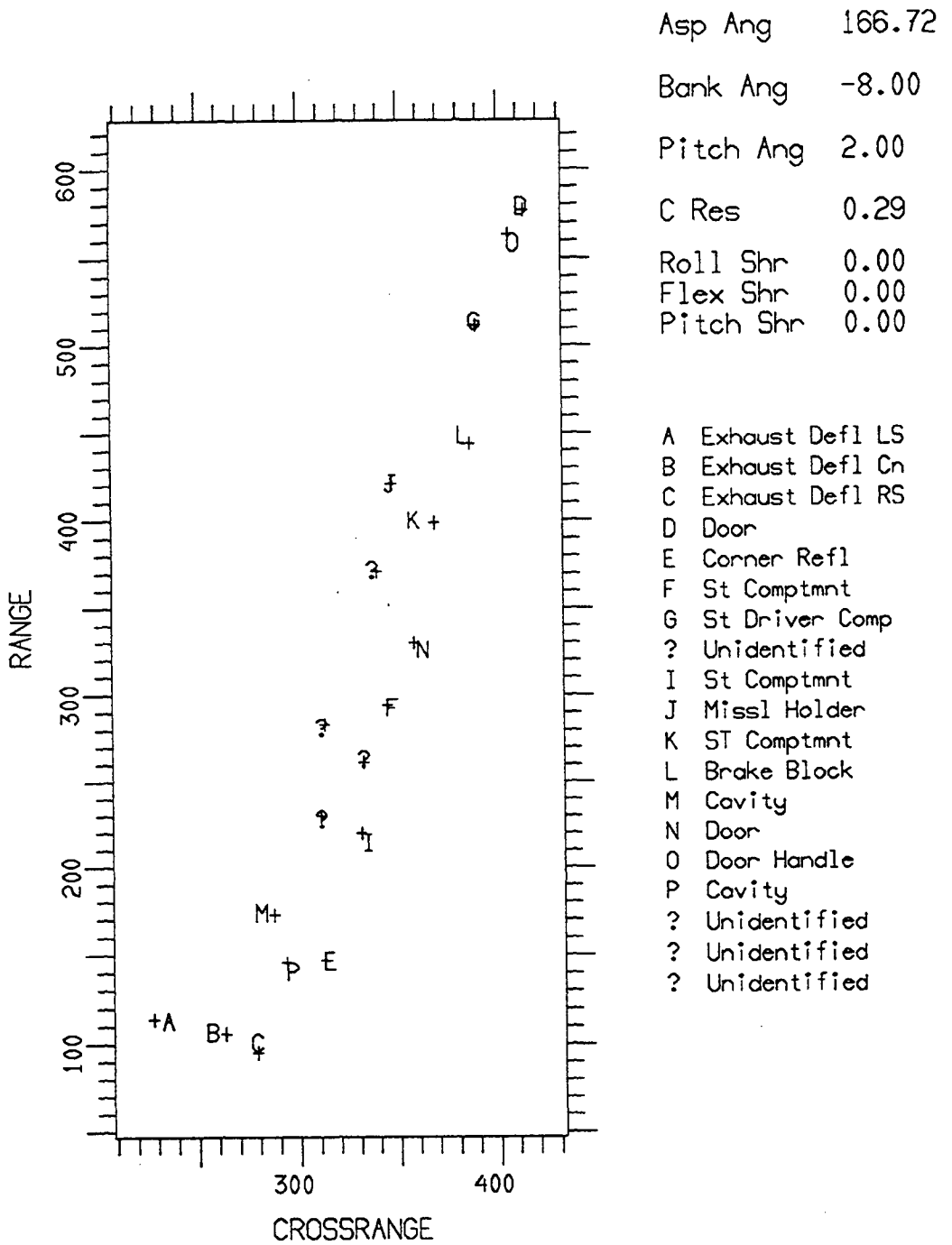

Figure 12. Positional Match for Imaging Interval from 0.19 to 0.36 s.

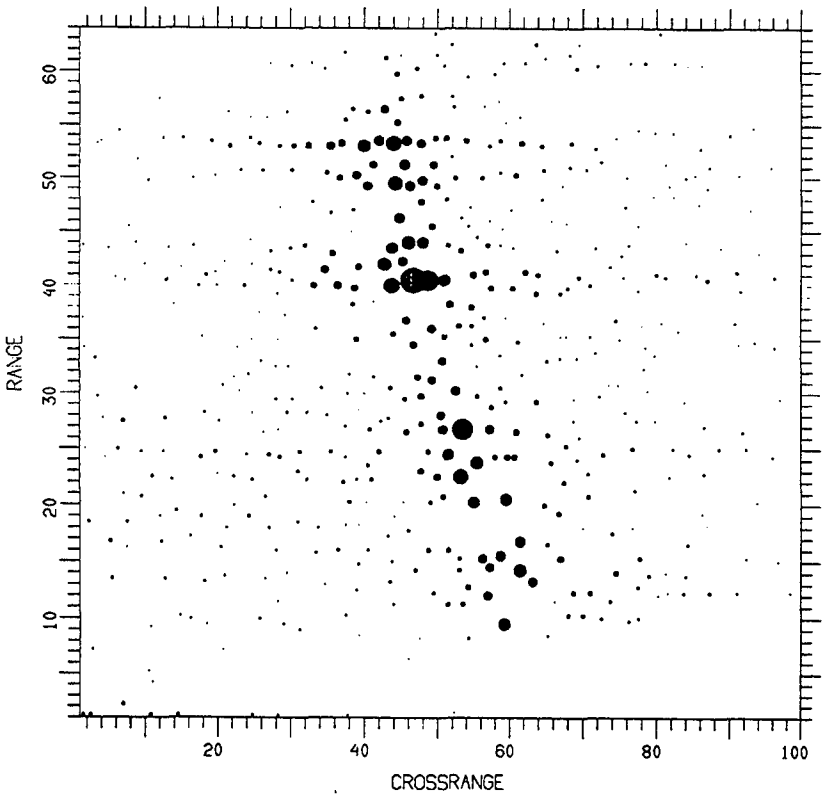

Figure 13. Image of TEL on Straight Smooth Road.

the vehicle have strong consequences. As concluded earlier, the processing and analysis of moving vehicles must be done adaptively, and this requires that the vehicle image be evaluated before deciding on the processing procedures. This means that we will examine several image cuts in different range gates spread over the length of the vehicle.

We select an image cut in the range gate of the first scatterer, Range Gate 9.59, and take the transform. The result is shown in Figure 14. The phase function has a break, and the two linear phase slopes correspond to crossrange positions that differ by about two gates (see the printout on the right margin, the item "slope"). If all scatterers had the same behavior, we could choose either the first or the second half of the imaging time, or alternatively correct the break in the phase function. The former approach was usable for the turning TEL, because the turning motion provided more than sufficient crossrange resolution with short imaging times. We can estimate to what degree the imaging time may be reduced in the present case.

We recognize from the crude image in Figure 13 that the width of the vehicle is in the order of five crossrange gates. Although we do not need high crossrange resolution when the aspect angle of the vehicle is small, five crossrange gates over the width of the vehicle is not so much that it can be

greatly reduced. A correction of the break in the phase slope would be more in order, provided it occurs for all scatterers.

In Figure 15 we show the analogous transform in Range Gate 26.80. The phase slope measurement shows the same type of break as in Figure 14 by about the same amount. However, in particular in the right half of the phase function we now observe a (significant) phase deviation of about 0.1 cycle, which is absent in Figure 14. The scatterer in this range gate thus contains a high-frequency motion component that was absent in the former scatterer. A common motion compensation for the entire vehicle thus appears inappropriate.

The same type of transform for the image cut in Range Gate 40.50 is shown in Figure 16. Although the rapid phase modulation in the right half of the figure is of the same kind as in Figure 15, for the left half the behavior of the phase function is quite different. Lastly, in Figure 17 we show the transform of the image cut in the last range gate on the vehicle, Gate 56.36. Again, there are some common elements in the phase function, but there are also differences.

From a comparison of the four phase functions we conclude that it is not possible to follow the crude motion compensation with one or more additional motion compensation steps for the vehicle as a whole and obtain an image of the quality needed for feature measurements, that is, for reliable vehicle identification. In principle, we must vary the motion compensation over the vehicle. This implies an undesirable processing complexity even when all scatterers in a given range gate have the same motion behavior. Since this need not be the case, the problem may be rather difficult, perhaps unsolvable.

In any case, before we resort to such a complicated motion compensation, we must be sure that a simpler approach is not workable. This is the approach we used with the TEL on a circle, where we selected such short imaging times that the consequences of the different motion behavior of the individual scatterers were acceptable. Although, as pointed out above, the approach is less applicable when the turning Doppler is small, in particular for the small aspect angle of the present TEL image, one must first evaluate the possibility of using this simple approach before resorting to a motion compensation that varies over the vehicle.

This evaluation consists of the following analysis. We take transforms over the range gates containing reasonably dominant single scatterers, such as represented by Figures 14 to 17, and ask the following question. Can we find a time segment over which the phases in all range gates are reasonably linear and have reasonably small deviations? Reasonably linear means that changes in

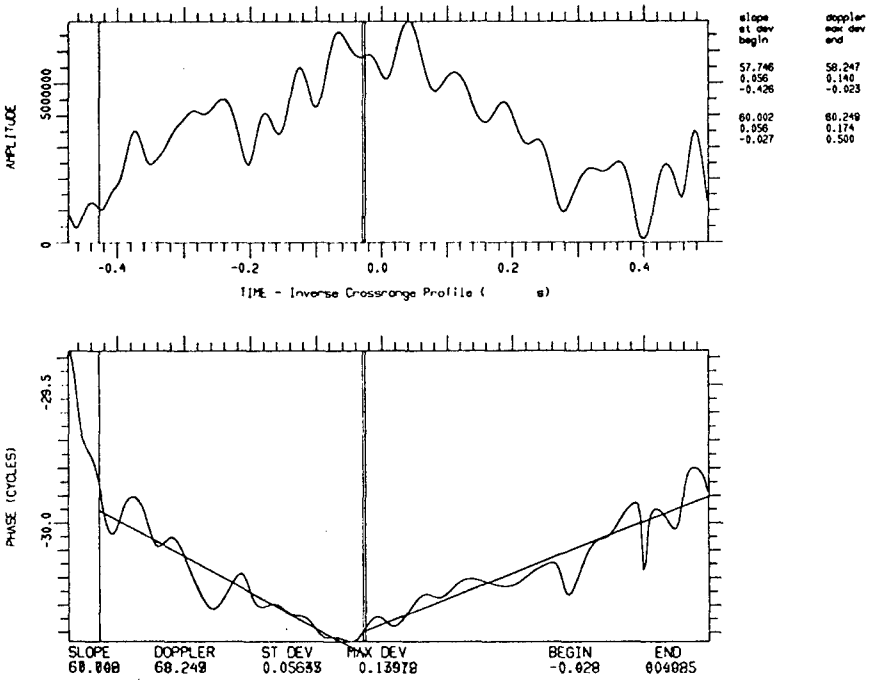

Figure 14. Transform of Image Cut in Range Gate 9.59.

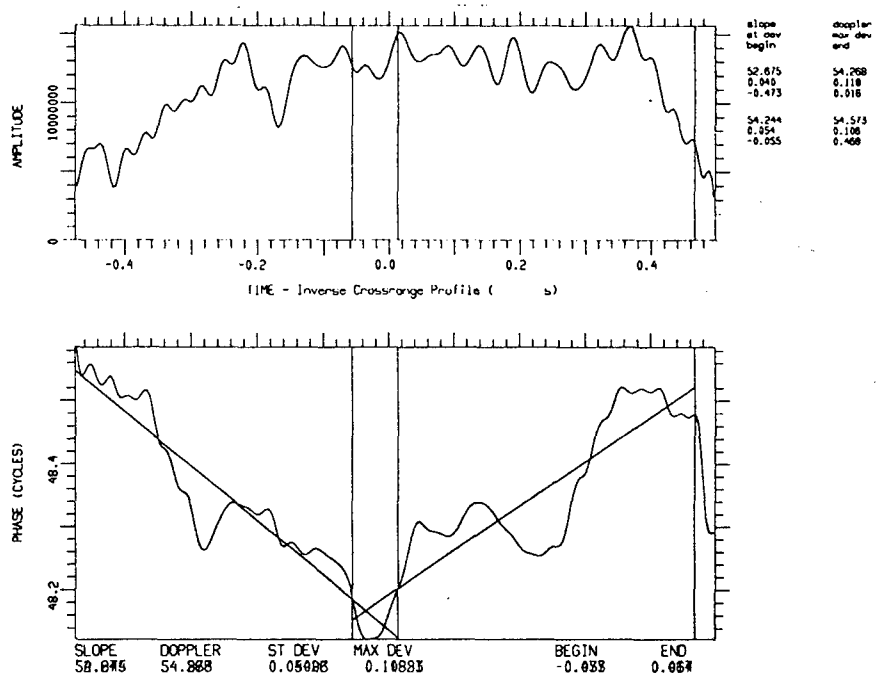

Figure 15. Transform of Image Cut in Range Gate 26.80.

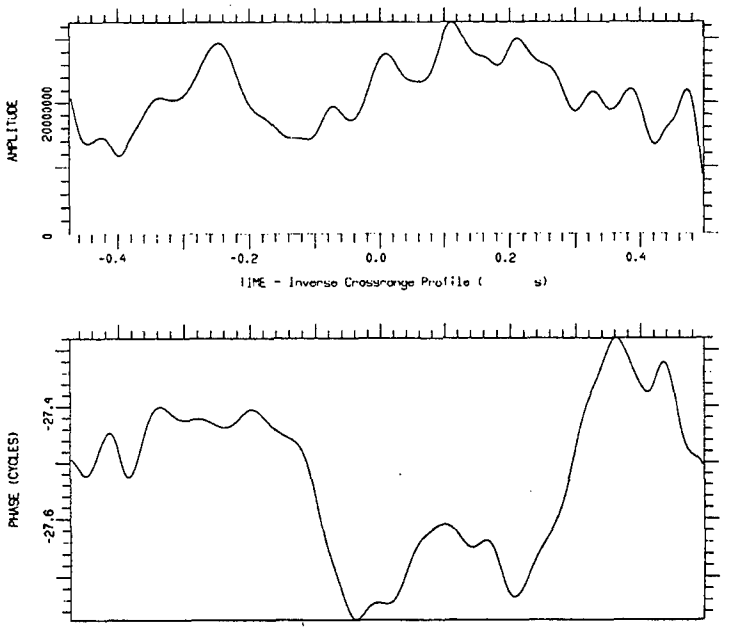

Figure 16. Transform of Image Cut in Range Gate 40.50.

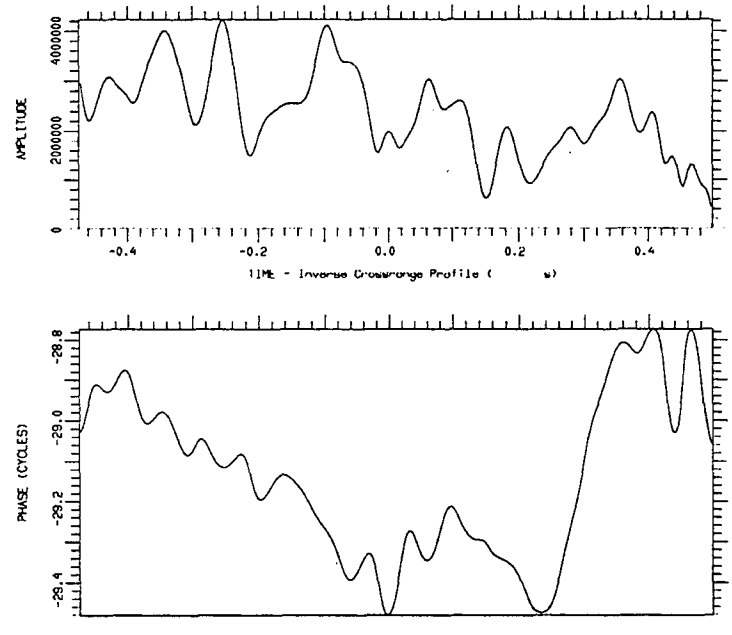

Figure 17. Transform of Image Cut in Range Gate 56.36.

the phase slope should amount to differences in crossrange gates that do not exceed about one gate. Reasonably small phase deviations are those that do not exceed about 0.1 cycles.

An examination of the phase functions in Figures 14 to 17 shows that the imaging interval from -0.4 to -0.1 s comes reasonably close to our requirements. This is not always the case at the fringes of this interval, but then the fringes are less important because weighting is used for Doppler sidelobe suppression. With the earlier estimate that the present image has about five crossrange gates over the vehicle width, use of the shorter imaging interval would reduce this number to between one and two. This appears acceptable, because range resolution is so high in this case that no crossrange resolution may be needed. The crossrange positions of the scatterers still will be measured to much better accuracy than the crossrange resolution (the position of a response peak can be measured to a small fraction of the response width).

An examination of Figures 14 to 17 also indicates that an inferior, but perhaps acceptable, processing interval might be from about -0.06 to 0.26 s. The phase function over this interval is quite linear in Figure 14. In Figures 15 through 17, on the other hand, there are phase modulations with a deviation of about 0.1 cycles superposed. Thus we would expect a somewhat worse performance than for the earlier interval. We will make the following test. We will derive a positional match for the first interval, and then match the measured scatterer positions for the second interval to the predicted scatterer positions for the first interval. Since the centers of the two intervals are separated only by about 0.7 s, any differences between the two positional matches should be due primarily to differences in the instantaneous motions.

The peaks plot image for the time interval from -0.4 to -0.1 s is shown in Figure 18. Relative to the image in Figure 13, the interesting point is that reducing the imaging time from 2 to 0.6 s has not eliminated the spurious responses generated by the "vibration" motion of the scatterers. Whereas for the TEL on a circle, in Figure 7, most of the responses are confined to the outline of the vehicle, while most of the spurious responses in Figure 18 are outside the outline. Note that in the latter figure the width of the vehicle extends only about three crossrange gates. This is a first indication that the mere reduction of the image time, as was used with the TEL on a circle, will not suffice.

An investigation of this point has revealed the following situation. In those cases where the motion compensation is satisfactory, as evidenced by the fact that there are few spurious responses due to the residual motion of the scatterers, we can use the processing methods developed for aircraft and also

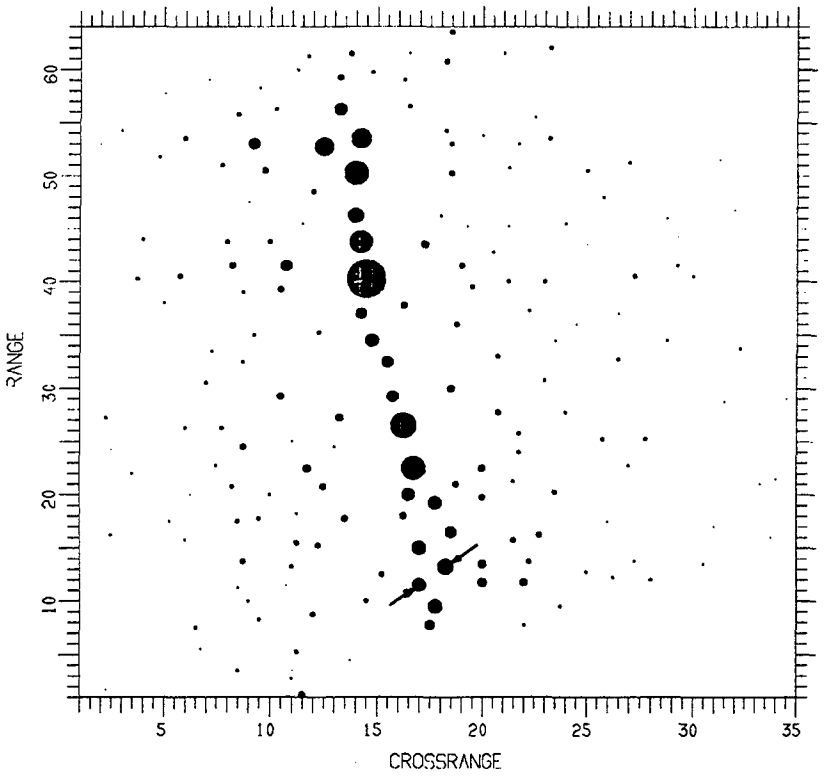

Figure 18. Image Over Interval from -0.4 to -0.1 s.

applied for the TEL on a circle. The cornerstone of these processing methods is the use of the complex image, rather than the intensity image, in order to achieve the inherent resolution capability of radar. When the intensity image is used, resolution in both range and crossrange are degraded by a factor of two. However, with the typical size of ground vehicles and the resolution available from practical radars, such a degradation of resolution is unacceptable. For this reason, we have had to extend our theory to the case where the scatterers have some residual high-frequency motion. Only after this extension did we obtain satisfactory positional matches. We will discuss this new procedure subsequently.

As an example, we consider the strong response in Range Gate 26.53. The image cut in the range gate is given in Figure 19. With a good motion compensation, we would place the transform window as marked in Figure 19, obtaining the transform in Figure 20. The amplitude and phase pattern would be interpreted as stemming from the interference between two scatterers, and the TSA algorithm can be used to determine the crossrange positions of the two scatterers [1]. Similarly, we would take an image cut in the crossrange gate of the response, shown in Figure 21. The transform window would be placed as indicated in Figure 21, giving the transform in Figure 22. This pattern again would be interpreted as an approximation of the interference pattern from two scatterers, and the TSA algorithm would give the scatterer positions in range.

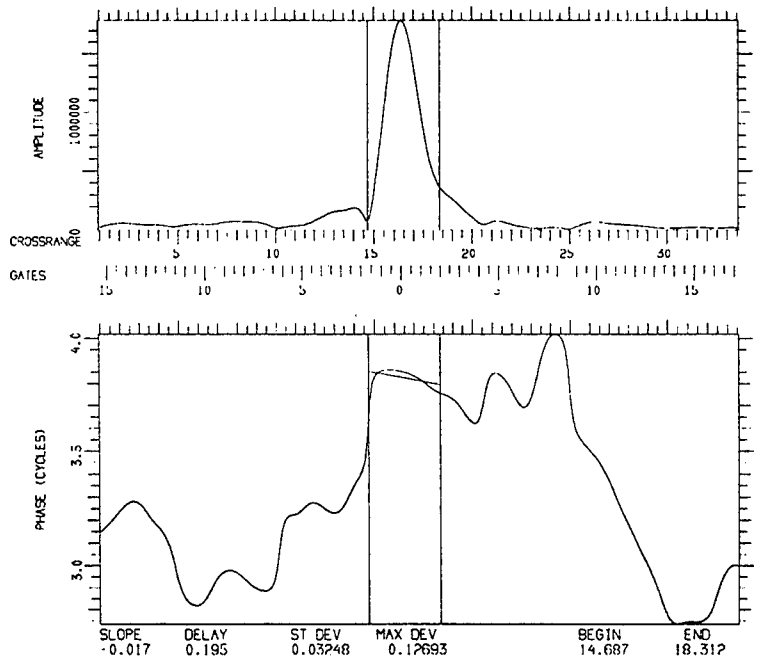

Figure 19. Image Cut in Range Gate 26.53.

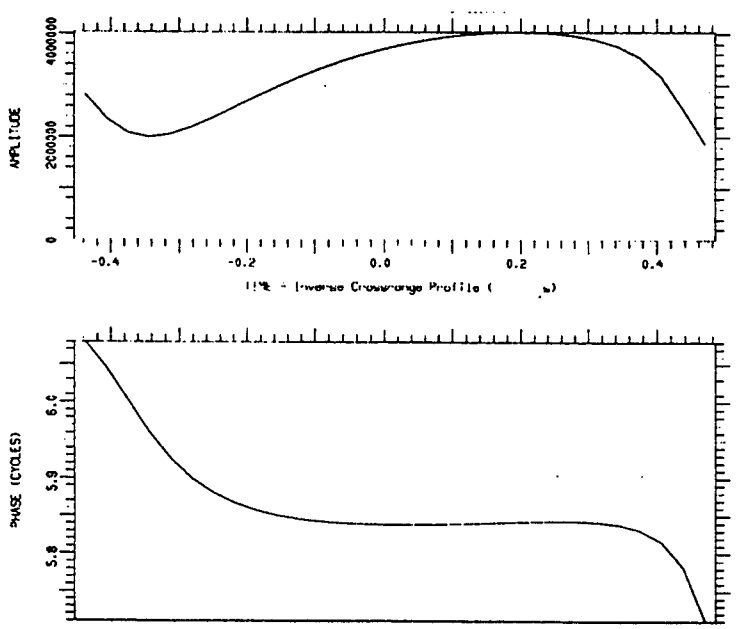

Figure 20. Transform Over Window in Figure 19.

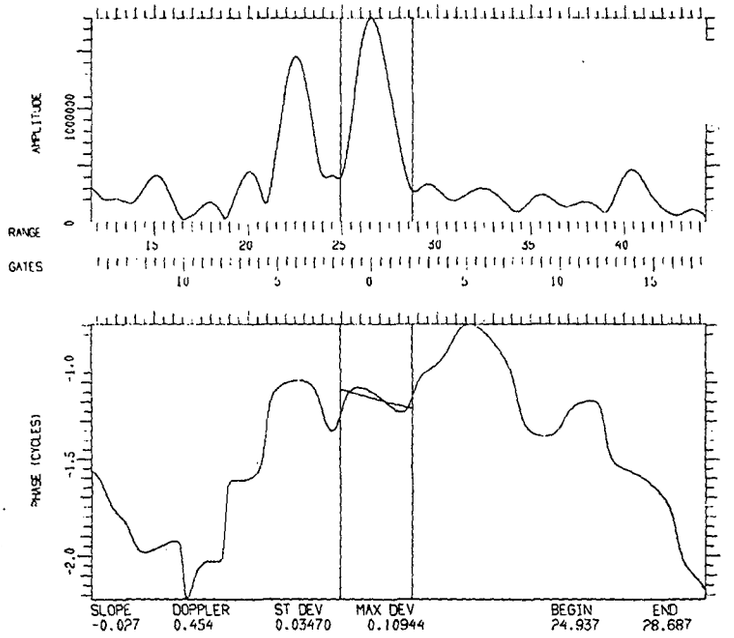

Figure 21. Image Cut in Crossrange Gate 16.35.

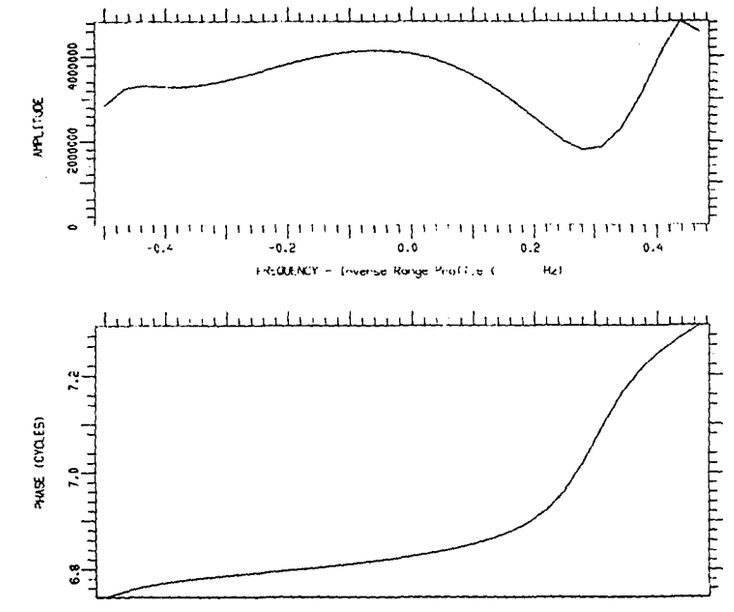

Figure 22. Transform Over Window in Figure 21.

In incompletely compensated images we cannot use the procedure without a prior test. We must first determine whether indeed two scatterers are present, in both the range and crossrange dimensions. We show the test first for the range gate of the response, that is, the image cut in Figure 19. Instead of taking the transform over the marked window, which is so narrow that all components due to a high-frequency motion are eliminated, we take the transform over the entire displayed interval. This transform is given in Figure 23. We can now reason that a single scatterer is present because the amplitude does not have any significant modulation. In this instance the phase function represents the motion of this scatterer, and we observe definite breaks in the phase slope. Measurements of the phase slopes reveal that they correspond to crossrange differences of one to two gates, the consequence of the residual scatterer motion.

For the analogous demonstration in the range domain, we would want to take the transform over the entire displayed interval in Figure 21. However, this test shows the intermodulation between the two strong responses in the image cut. Thus we place the left boundary of the transform window in Range Gate 24, with the right boundary at the right end of the image cut. The resulting transform is shown in Figure 24. This again is the amplitude/phase pattern of a single scatterer, or perhaps two scatterers so close to each other that they cannot be resolved. The conclusion is that we must not apply the TSA, but assume a single scatterer whose position is given by the position of the response peak. Note that, for purposes of target identification, it is very important not to interpret the response from a single scatterer as the combination of responses from two scatterers that are separated by much more than the acceptable small fraction of a gate.

The case just illustrated is relatively benign, although important. We will now illustrate a more drastic case, considering the two responses marked in Figure 18. If we analyzed the two responses on the assumption of a good motion compensation, we might obtain two, three, or four scatterers; we have not checked. Instead, we take an image cut along the line connecting the two responses, with the result shown in Figure 25. If this response were due to two scatterers, the transform would give the known amplitude and phase pattern from two scatterers. Instead, we obtain the transform in Figure 26. The amplitude pattern implies that there is a single scatterer that is fully visible only for a short period, and then its crossrange position is given by the phase slope. It is clear that an incorrect interpretation of the image responses would not permit the measurement of feature positions. It would not merely degrade the matching results, it would ruin them so that no reliable identification would be possible.

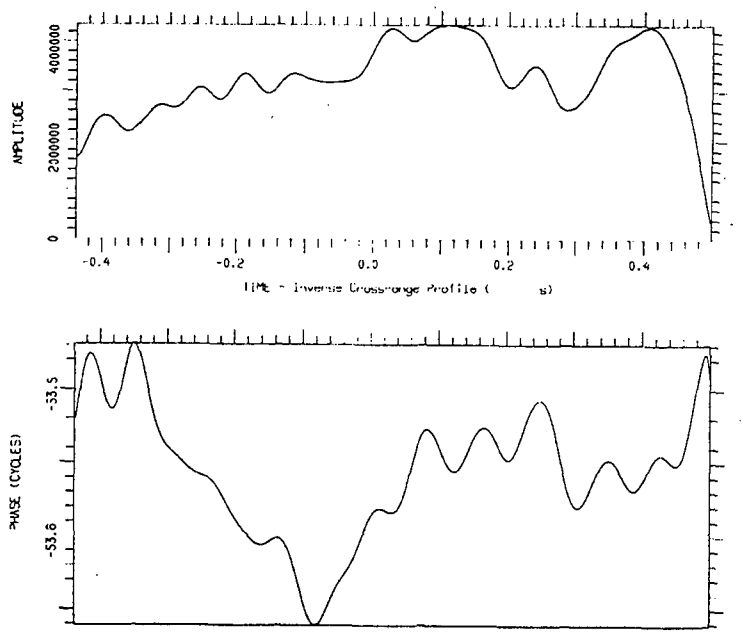

Figure 23. Transform Over Entire Displayed Interval in Figure 19.

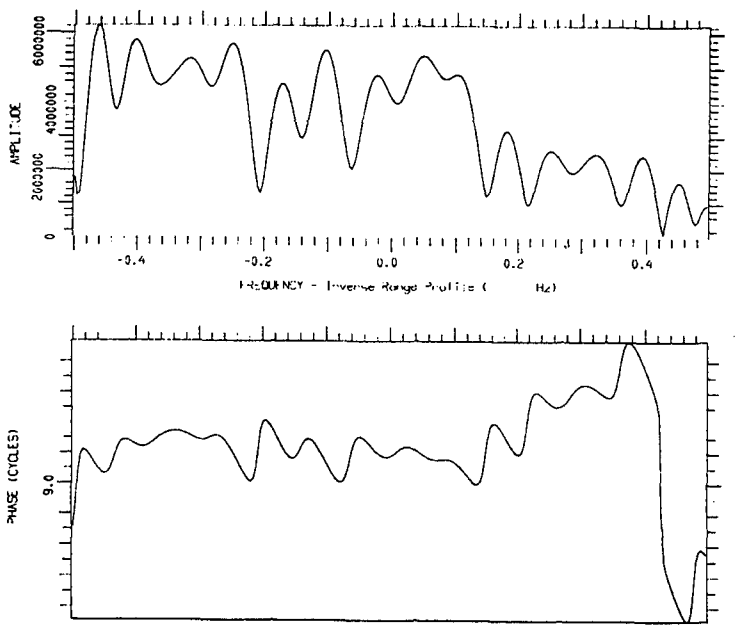

Figure 24. Transform of Image Cut in Figure 21 Between Gates 24 and 44.

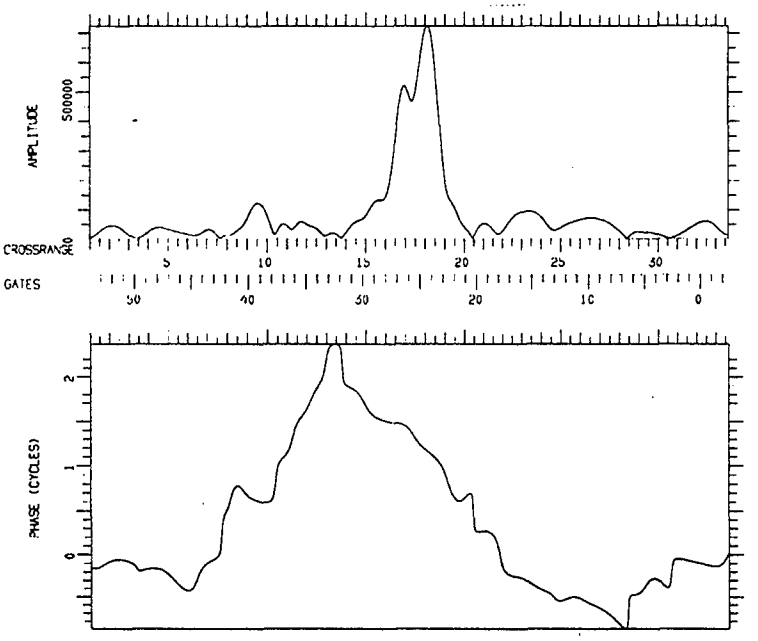

Figure 25. Image Cut Along Line Through the Two Peaks Marked in Figure 18.

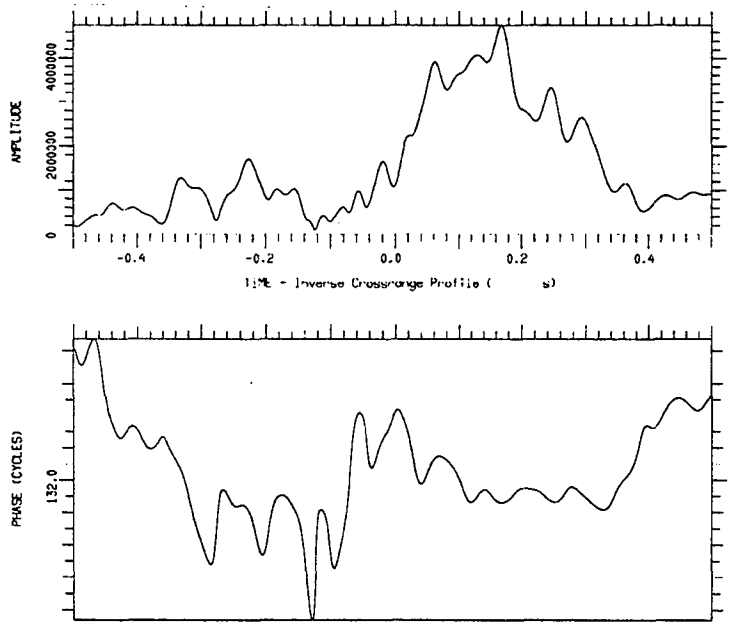

Figure 26. Transform of Image Cut in Figure 25.

We have used the appropriate checks on the responses, and then performed the measurements correspondingly. This yielded a set of measured scatterer positions from Figure 18. We examined the available diagrams of the TEL to determine the scatterers that should be visible for such a small aspect angle, and estimated their positions in three dimensions. The match between the measured and predicted scatterer positions is given in Figure 27. Because of the incomplete motion compensation, we allowed a larger measurement error in crossrange than in range. A point-by-point examination of Figure 27 shows a remarkably good match. There are differences, perhaps caused by measurement errors or the difficulties in interpreting the available diagrams of the TEL, but the match appears to be more than adequate for vehicle identification.

As already indicated, we made the same measurements on the image generated from the time interval between -0.06 and 0.26 s. The corresponding image is given in Figure 28. A comparison of the images in Figures 18 and 28 makes it obvious that one could not simply take the peak positions as the scatterer positions, since both images then would have to be nearly identical. If the indicated measurement procedures are used to determine the scatterer positions from the new image, and the measured positions are matched to the predicted scatterer positions used in the match in Figure 27, we obtain the result in Figure 29. The match is still very good, but not as good as in Figure 27. This was expected because the motion behavior of the vehicle is not as good over the second interval. Nevertheless, even the match in Figure 29 should suffice for vehicle identification.

We considered the TEL moving in a circle and the TEL on a straight smooth road, and showed that we can obtain a good positional match for both motion characteristics. This means that the different motion characteristics do not prevent us from measuring the same scatterer positions. Are these the same scatterer positions that one would also measure on a stationary TEL? They must be, if our entire philosophy of target identification is correct. For this reason, we chose an image of the stationary TEL at approximately the same aspect angle used for the moving TELs. We extracted the scatterer positions from the image and performed the positional match with the same database that was used for the preceding two positional matches. The result is shown in Figure 30. Because of the importance of this test, we will discuss the match in more detail.

Starting with the front row of scatterers, the stationary vehicle shows one additional scatterer, which has the position of the left corner of the bumper. It is not surprising that we can observe a weak scatterer on a stationary vehicle but not on a moving vehicle. The other matches are for the most part extraordinarily good. We do not have a response at Scatterer

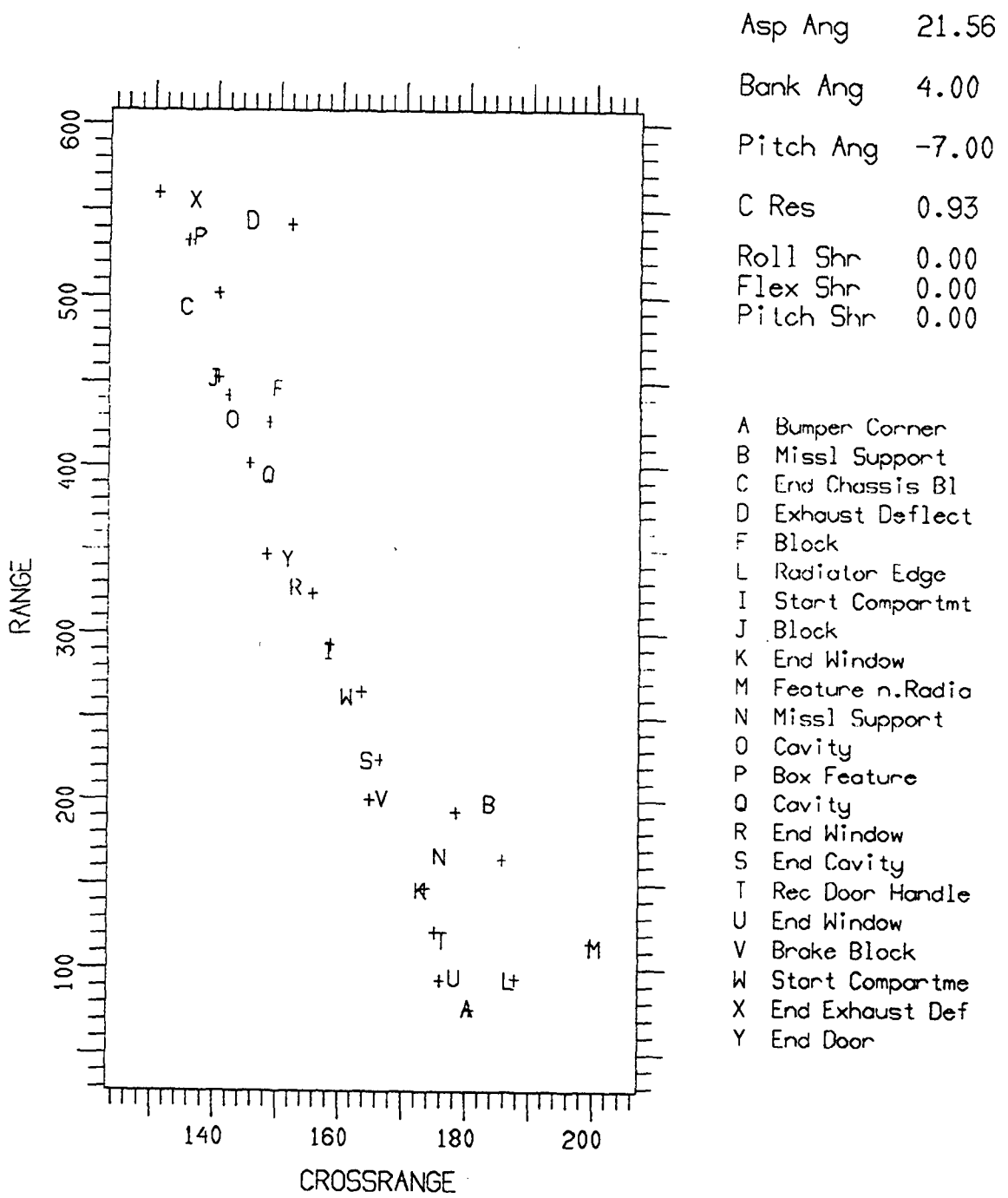

Figure 27. Positional Match for TEL Image in Figure 18.

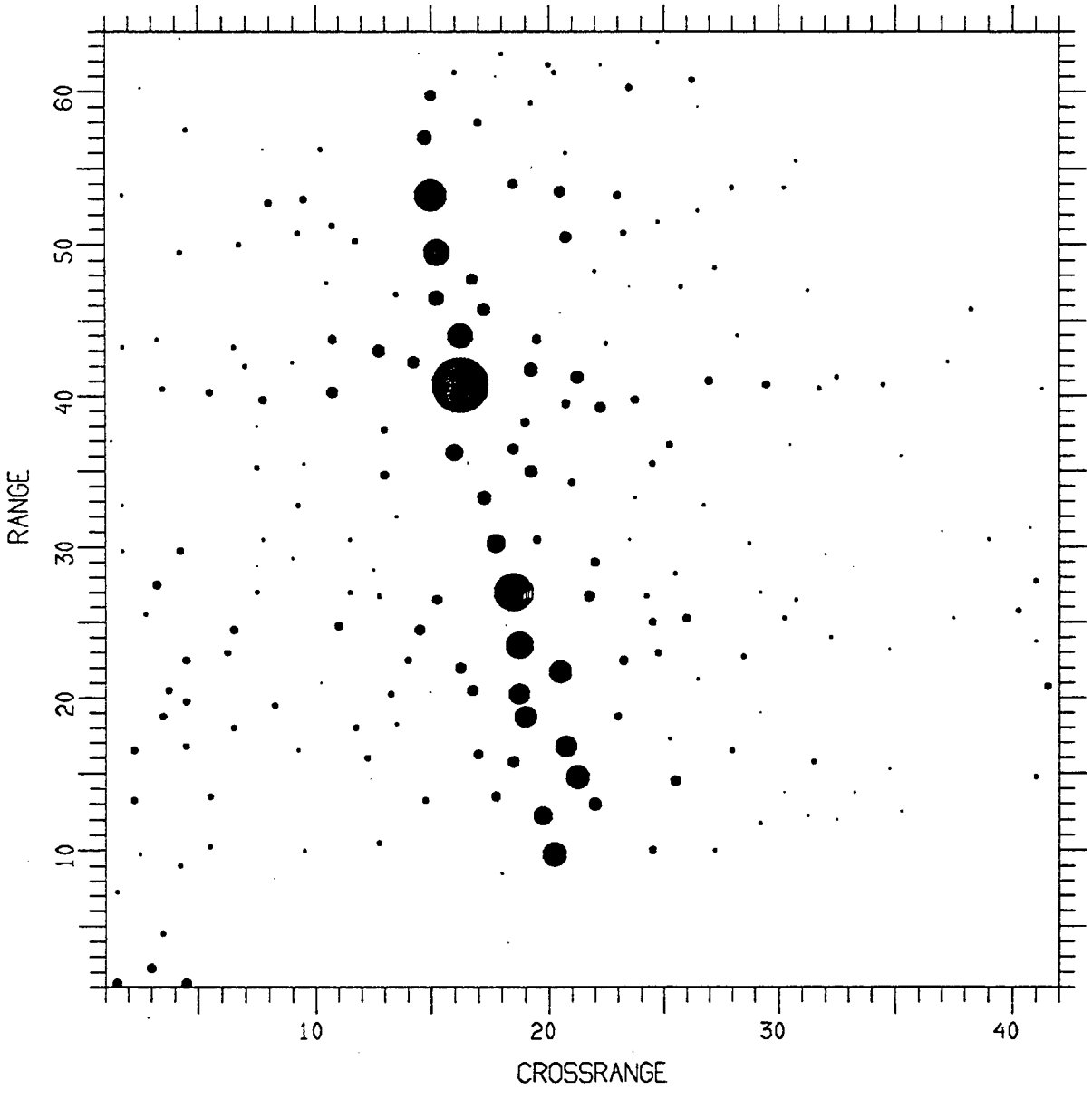

Figure 28. Image Over Time Interval from -0.06 to 0.26 s.

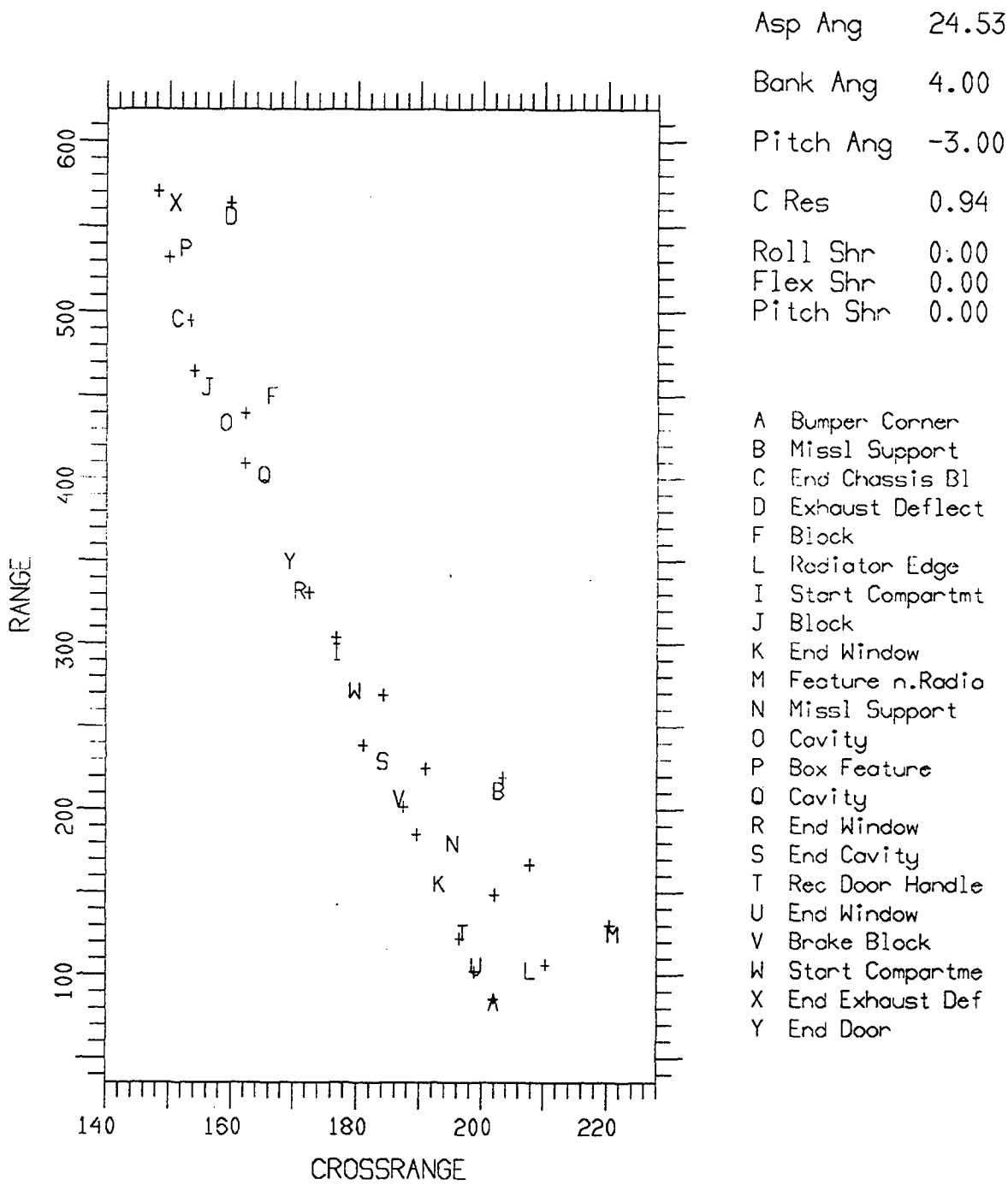

Figure 29. Positional Match Between Scatterer Positions Extracted from Figure 28 and Predicted Positions Used in Figure 27.

Position B, but there is an additional response to the right of the S. Since we have inadequate information for the top view, we have not seriously tried to match positions in the vicinity of the missile. The differences observable for some scatterer positions can be traced to interference from strong responses, which causes unavoidable measurement errors or even the loss of weak responses. Overall, however, the positional match between the scatterers extracted from the image of the stationary TEL and the database of the moving TEL is very good, by far better than what is needed for reliable vehicle identification.

2.3 The TEL on a Bumpy Road (Data Sets dra030500a006 and dra030500a011)

The vehicle traveled on a road that contained a set of deep ruts, a set of dips, and a set of speed bumps, in this order. As we do not have data for the entire trip down the road, we did not try to determine for which data files the TEL went over each of these ruts. Instead, we looked for images with the largest degree of crossrange spread, an indication of poor quality. We then selected the worst for analysis. Later we found images of even worse quality, which we also examined.

In Figure 31 we show the peaks plot image over an interval of 2 s and centered at the time of 70 s. As was done with the earlier images, the only kind of motion compensation that was used is a smooth range and Doppler compensation on the vehicle as a whole, which is the "standard" compensation. This image does not show any significant spread in crossrange, indicating that the TEL apparently has not yet reached the ruts. In Figure 32 we show the same type of image 2 s later, with severe smearing in crossrange (this and the following two images were inadvertently flipped in crossrange). The image another second later is shown in Figure 33. In comparison with Figure 32, the smearing in crossrange is now less severe. Another second later we obtain the image in Figure 34. The smearing is further reduced. The worst motion of the TEL thus occurs at the time of 72 s, and we selected this worst case for analysis. To accommodate the severe shaking of the TEL, we again had to somewhat modify or extend our processing and analysis procedures. However, as will be seen below, a simple test will tell us what kind of procedure is needed, so that there is no problem in implementing the processing adaptively.

For the images in Figures 31 through 34, we suppressed all responses that are more than 20 dB below the highest peak of the image. Consequently, one cannot appreciate how poor the images really are. In Figure 35 we show the selected image on an expanded scale and with less severe clipping of the lower-level responses. As always with a moving target, the question is whether one could improve the motion compensation so that the image becomes

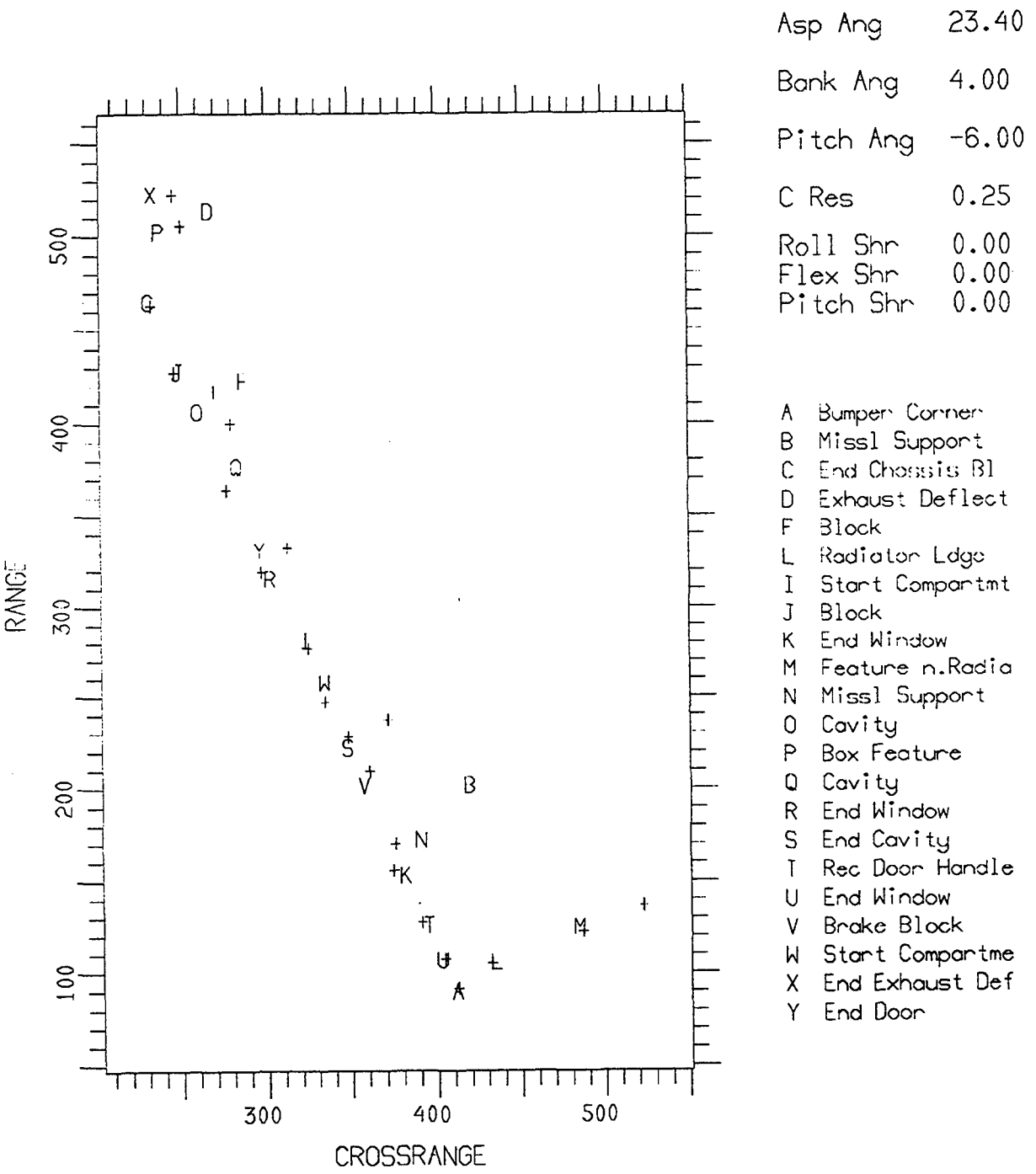

Figure 30. Positional Match Between Measured Scatterer Positions for Stationary TEL and the Database for Moving TEL.

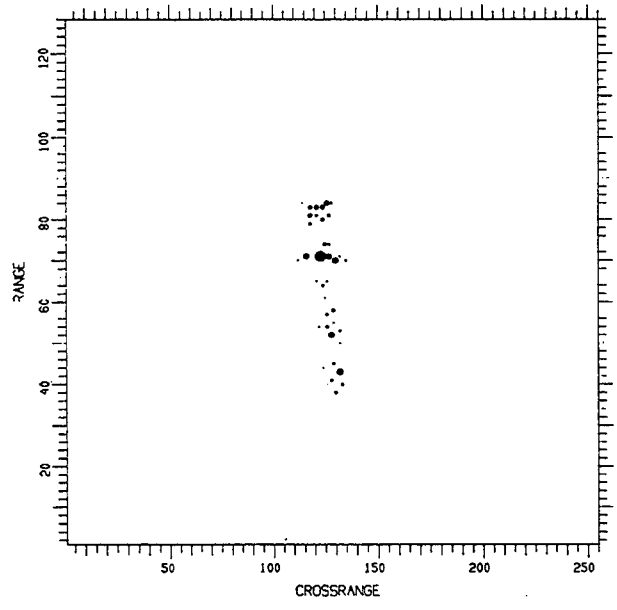

Figure 31. Image at Time of 70 s.

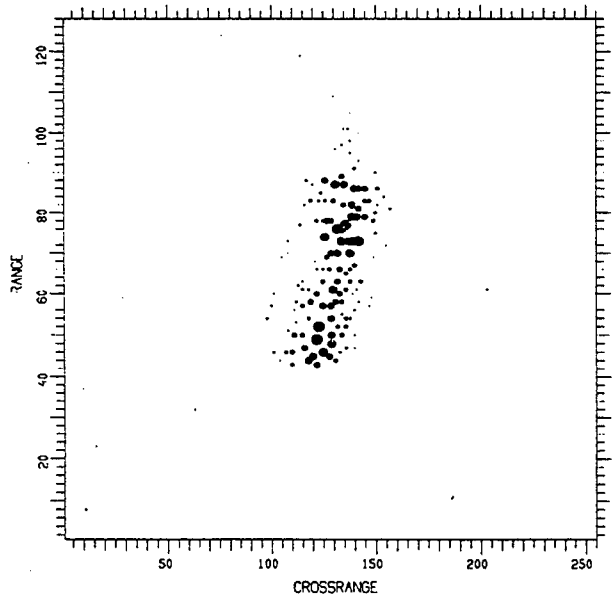

Figure 32. Image at Time of 72 s.

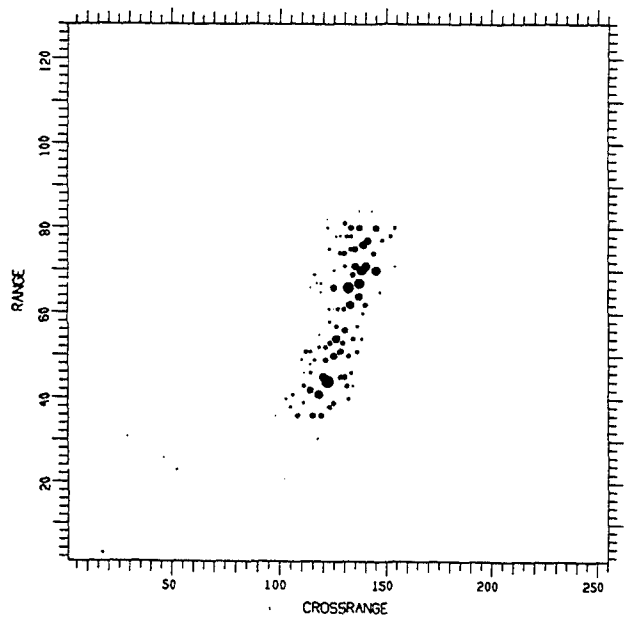

Figure 33. Image at Time of 73 s.

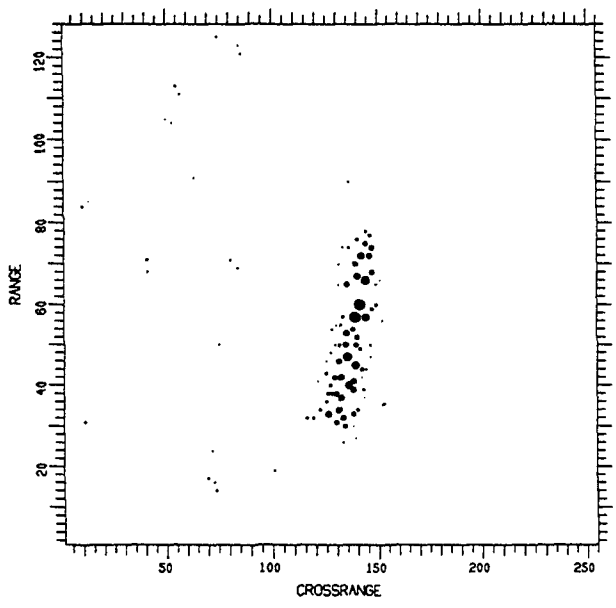

Figure 34. Image at Time of 74 s.

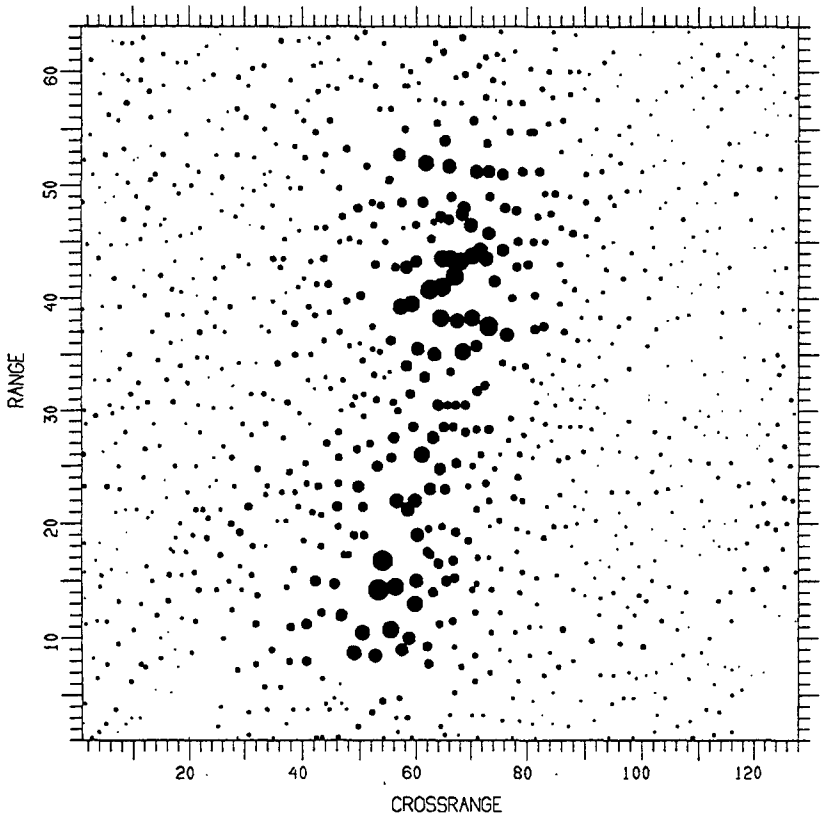

Figure 35. Image in Figure 32 on an Expanded Scale.

well focused. It will become evident that the answer is no, much more so than with the TEL on a smooth road. Of course, we cannot prove that a good motion compensation is impossible; but at this time we see no way of compensating the different vibrating components of the TEL.

When one obtains an image, the first task in the analysis is to understand it. This first step is done by examining range gates throughout the vehicle. We will do this subsequently to explain the method. However, this is not merely necessary to obtain a general understanding of the behavior of such a vehicle and to decide on some way to analyze the image. The very same procedure must also be implemented when the images are evaluated fully automatically. There is a range of processing options, and a decision to use a particular option must be made automatically in an operational system.

For the analysis we will always examine range gates in which a single scatterer appears to be dominant, as indicated by a single strong peak in a given range gate, or perhaps by an isolated peak that may not be so strong. Our limited experience with such data indicates that the backscattering from ground vehicles is typically concentrated at their leading edges, which facilitates finding a range gate with a dominant scatterer. Otherwise we may have to reduce the imaging time in order to reduce the crossrange smearing of

the individual responses in each range gate. In Figure 35, we will start with what appears to be an isolated peak at the closest range, at about Range Gate 7.5. The image cut in the appropriate range gate is shown in Figure 36. Image cuts are difficult to evaluate directly, unless one scatterer is truly dominant. Thus we usually take the transform of the image cut, as given in Figure 37. Since dominance of a scatterer implies that the amplitude has a low percentage modulation, we find that Figure 37 contains only short periods of scatterer dominance, all in the second half of the time interval. Thus we observe just one or a few scatterers, but only for short periods of time. Specifically, we can claim to observe a scatterer if a section with little percentage amplitude modulation coincides with a linear or a smoothly curved phase. The phase deviations from a straight line must not exceed the order of 0.1 cycles, which is equivalent to requiring a small percentage amplitude modulation. Since Figure 37 is a poor example of the transform of an image cut, we will give more explanations in connection with other image cuts.

The image cut in Range Gate 16.72 is shown in Figure 38, and its transform is shown in Figure 39. The latter figure clearly shows that a scatterer becomes dominant around the normalized time of -0.2 s. A strong amplitude with weak modulation coincides with a linear phase function. Since linear phase implies a constant Doppler, the slope of the phase function gives the crossrange position of the scatterer. The amplitude/phase pattern implies that the following situation exists with the TEL: aside from the translational motion of the vehicle, which is the basis for SAR/ISAR imaging, the various scatterers have additional motions that, in want of a better name, we call vibrations. If a scatterer has a vibration motion large enough to induce a significant phase modulation, the scatterer response will be focused only at the times at which the vibrational motion is one of constant range rate. At other times the scatterer response will be smeared into the background. Thus we obtain only glimpses of a scatterer. If at the time of constant range rate the value of the range rate happens to be zero, the response will appear in the correct crossrange position. If the range rate at the time of sufficient constancy happens to be nonzero, the scatterer response will be translated in crossrange from the position of the scatterer. If the phase slope changes during the time of scatterer dominance, as it does in Figure 39, the scatterer is being observed at different range rates.

In Figure 40 we show another image cut in Range Gate 25.96. The transform is given in Figure 41. As given by the interval marked by the crosshairs, in this particular range gate the periods of strong scatterer dominance are quite short. Note that there is a minimum period for defining scatterer dominance and phase slope, this minimum being in the order of five

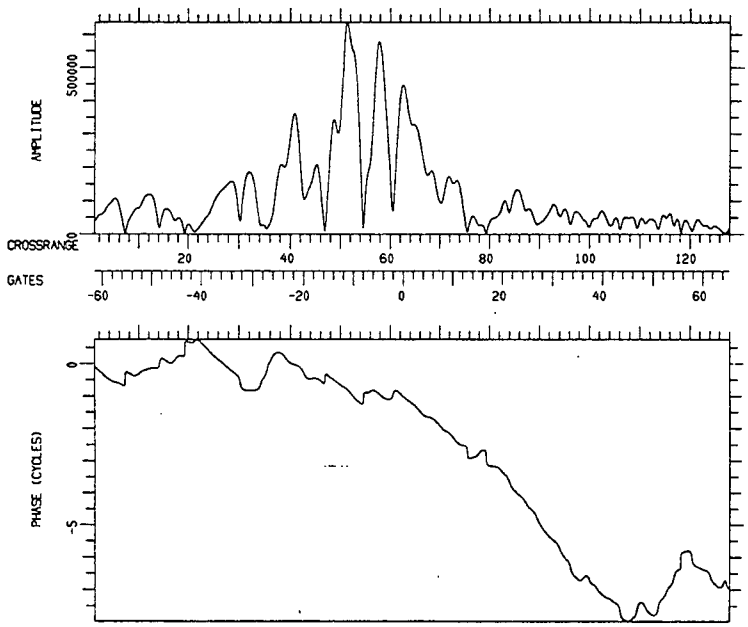

Figure 36. Image Cut in Range Gate 7.28.

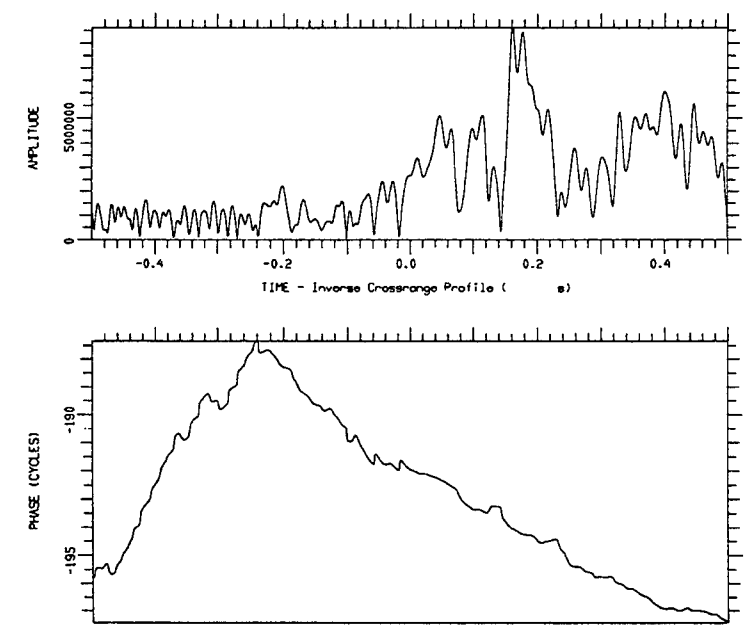

Figure 37. Transform of Image Cut in Figure 36.

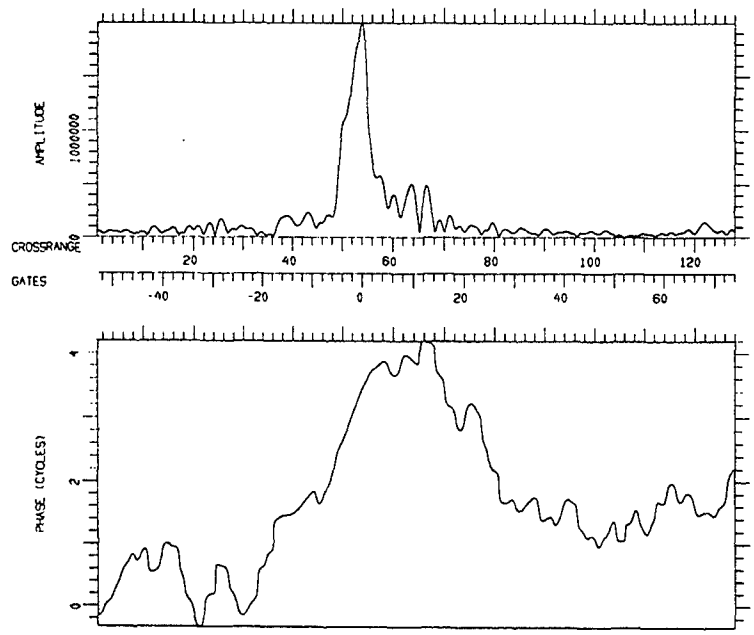

Figure 38. Image Cut in Range Gate 16.72.

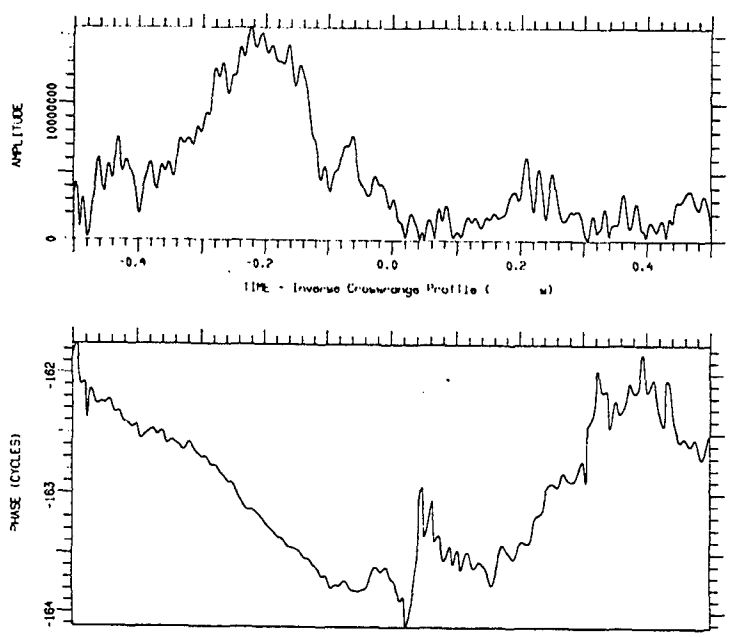

Figure 39. Transform of Image Cut in Figure 38.

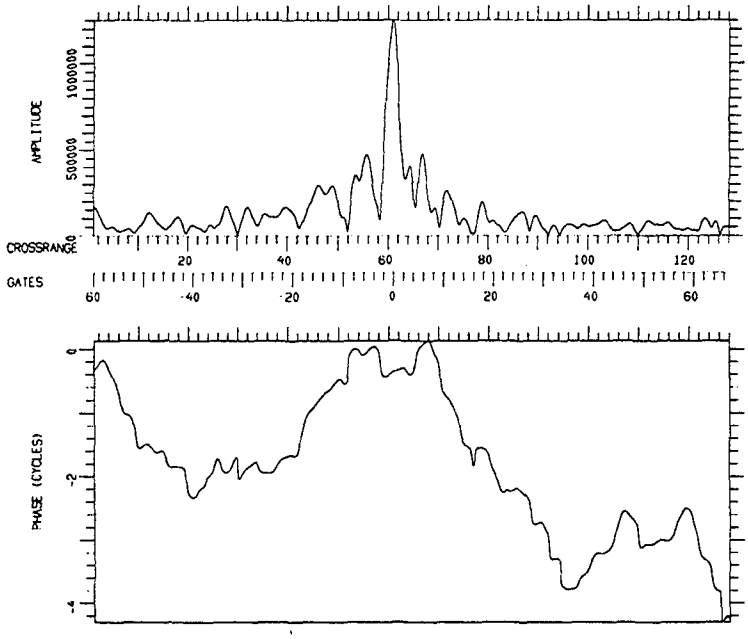

Figure 40. Image Cut in Range Gate 25.96.

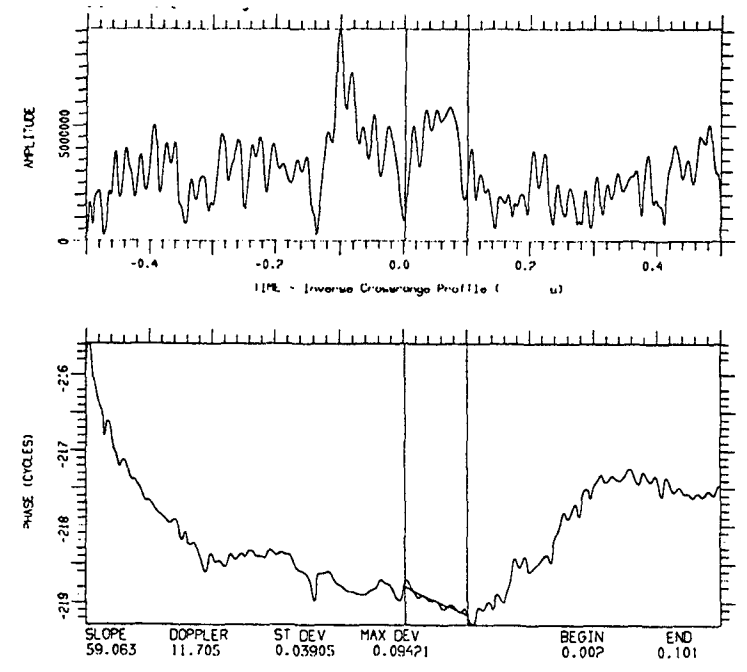

Figure 41. Transform of Image Cut in Figure 40.

fluctuation cycles. In other words, unless the segment of "linear" phase contains at least about five fluctuation cycles, the definition of phase linearity becomes meaningless.

As another illustration, in Figure 42 we show the transform of the image cut in Range Gate 37.61. The period of major scatterer dominance is not only short, but it splits into two parts with different phase slopes (different range rates of the scatterer). The printout on the right margin gives the phase slopes as corresponding to Crossrange Gates 69.39 and 74.75. This is a crossrange difference of more than five gates. The implication is that the range rate of the scatterer changes abruptly to cause a very large change in the crossrange position of the response. At the end of the time period, we also observe a scatterer at a still different crossrange position.

To show the large variations of the situation over the range gates, in Figure 43 we show the transform of the image cut in Range Gate 41.83. We again observe different periods of dominance, at different times and of different durations, with corresponding linear phase slopes. As a last illustration, in Figure 44 we show the transform of the image cut in Range Gate 51.15. Not only is there a single short time of scatterer dominance, but during this short time the phase slope breaks and indicates scatterer positions almost five crossrange gates apart.

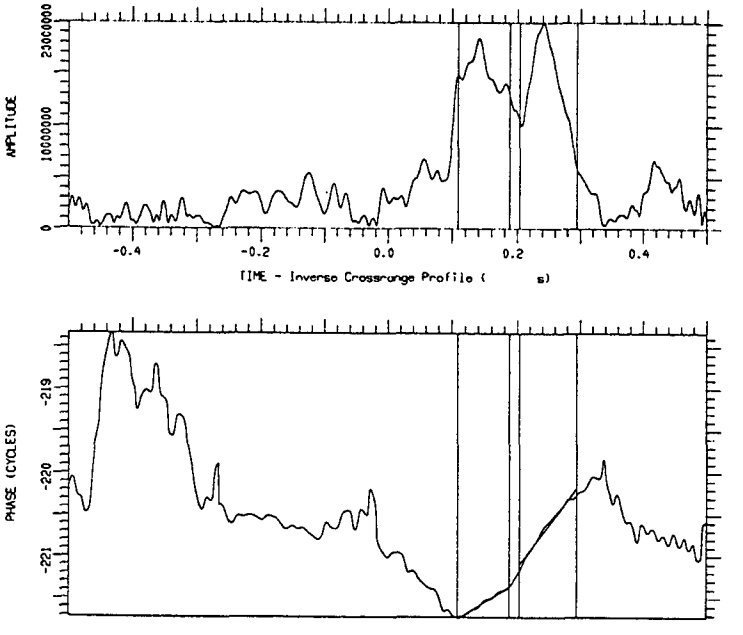

Figure 42. Transform of Image Cut in Range Gate 37.61.

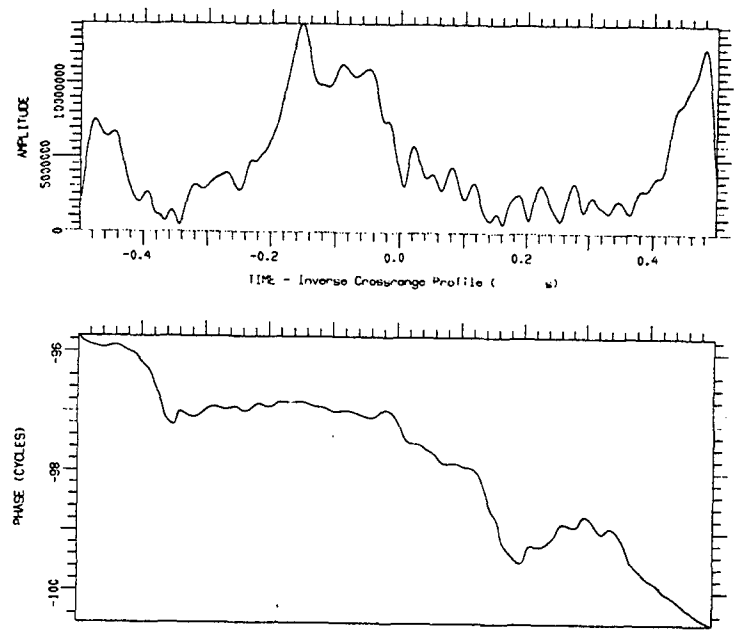

Figure 43. Transform of Image Cut in Range Gate 41.83.

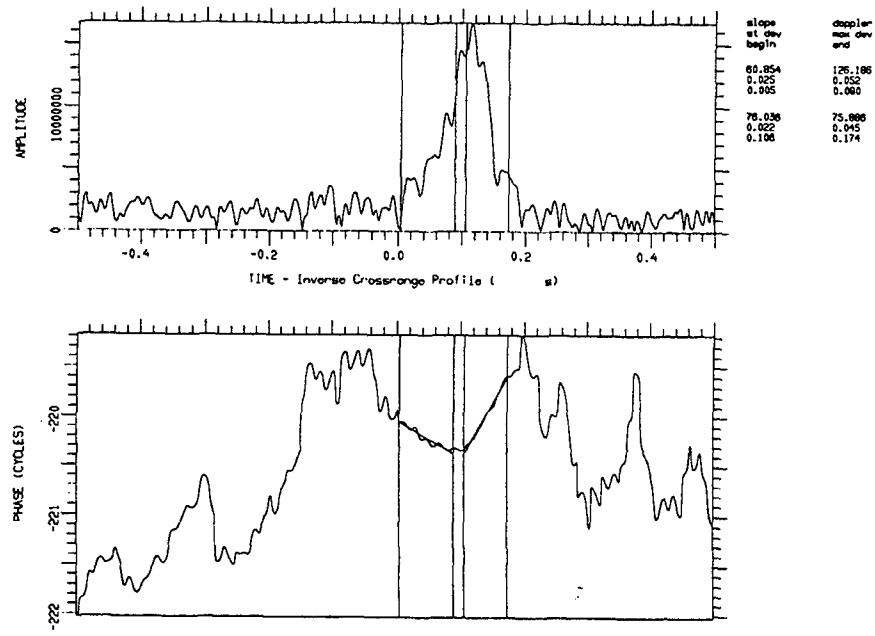

Figure 44. Transform of Image Cut in Range Gate 51.15.

Interpreting the preceding examples, we have the following situation. Different parts of the TEL have different vibrations, both in magnitude and timing. A scatterer in a given range gate might be moving at a constant range rate over a substantial part of the observation interval, in which case there will be a long period over which it can be observed. The time interval over which the range rate is essentially constant might be much shorter, or it might be so short that the scatterer response will not be observable in the background at all. During a period of scatterer dominance the phase slope might or might not remain the same, so that the apparent scatterer position might or might not change. In effect, the scatterers in different range gates have rather different behaviors that make them more or less difficult to observe.

In principle, we could measure the motion behavior of each major scatterer, determine its average Doppler, and then find its crossrange position as if the vehicle were stationary. Based on our general experience in this field, we believe that this is impossible in practice. In other words, we do not believe that is feasible to develop a good enough motion compensation that ultimately would reduce the analysis of the image to that of a stationary vehicle. Rather, we must perform the required image analysis despite the poor motion compensation. We examine range gate by range gate, search for the periods of scatterer dominance, and during these periods we measure the crossrange positions of the dominant scatterers. We accommodate the uncertainty in the crossrange position of a given scatterer because of its irregular motion by allowing a large crossrange uncertainty in the positional match. Crossrange resolution or, more precisely, a long observation interval still is very useful because it greatly increases the chance of observing scatterers. Utilizing the different timing of scatterer dominance is an indirect way of utilizing crossrange resolution despite the fact that the range rates of the scatterers do not remain constant.

One question is whether, in a given transform of an image cut, we utilize only the periods of major scatterer dominance, or also the periods of minor dominance. Our philosophy is that the number of scatterer positions needed for positive vehicle identification is not large, so that only the best measurements should be used. There still remains the question as to how the range positions of the scatterers should be measured, with the crossrange positions determined from the phase slopes in the transforms of the image cuts in range gates.

We have solved this problem, but perhaps not in the most efficient manner. With the procedures formulated during this program, we select a range gate, and from the transform of the image cut in the range gate we determine

the major period of dominance. Then we generate a short term image over the period of dominance, and determine the range position of the scatterer by taking the transform of the response in its crossrange gate, and using one of the following procedures. If the relative half-power width of the response is so close to unity that we would choose the peak position as the position of the scatterer for a good motion compensation, we do likewise. However, we verify the measurement by taking a transform and confirming that the phase is linear over essentially the full spectrum. If it is not, then we measure the phase slope over the interval within which it is constant, and choose that phase slope rather than the peak position as the measured range position of the scatterer. If the relative half-power width is so large that we would normally use the TSA to determine the scatterer positions, we do the same. However, we require the amplitude/phase pattern to be a better approximation of the ideal pattern than when we know the compensation to be good. Otherwise, we search for linear phase slopes in order to determine the scatterer positions.

These phase slope measurements can be performed only if the response is sufficiently isolated to allow using a relatively wide transform window. If this is not possible and the pattern of the transform is too poor for acceptable measurements, we use the peak position. These types of measurement are performed in all range gates with major scatterers. In cases where the time intervals of dominance overlap for different range gates, the same short term image is utilized for these range gates. Note, however, that we did not have the time to develop fully defined rules, as needed for automating the measurements.

We will now illustrate the process. Choosing the example in Figure 39, we find that in Range Gate 16.72 a scatterer is well dominant within the time interval from -0.29 to -0.12 s. The image over this particular time interval is shown in Figure 45. Note that the scatterer response in Range Gate 16.72 has become one of only three strong responses, with the range gate shifted somewhat. The three strong responses come from the scatterers to which the chosen imaging interval happens to be well matched. To measure the range position of the scatterer, we take an image cut in the crossrange gate of the response, as shown in Figure 46. In this particular instance the response peak does appear close to the correct position, but in general we cannot be sure. If the TSA should prove unreliable in such an instance, in order to measure the range position we take the transform over an interval that is chosen so as to exclude most of the interference on one side of the response, without cutting off too much of the response of interest. With the choice of the left boundary as indicated in the figure, we obtain the transform in

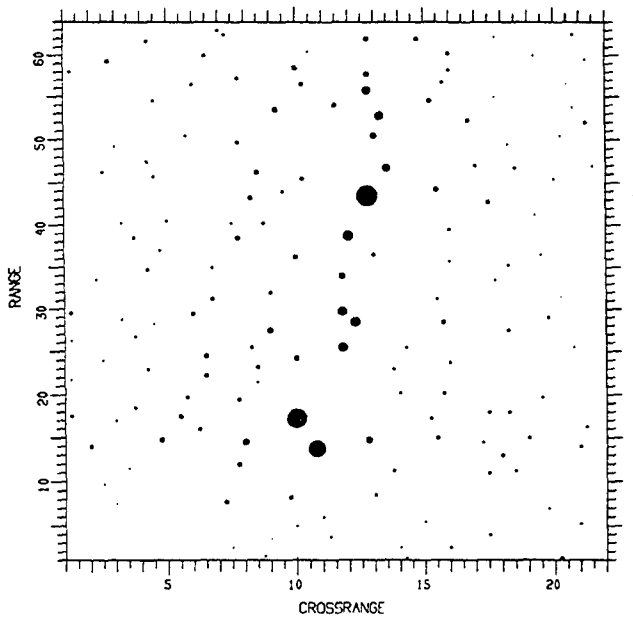

Figure 45. Image Over Time Interval from -0.29 to 0.12 s.

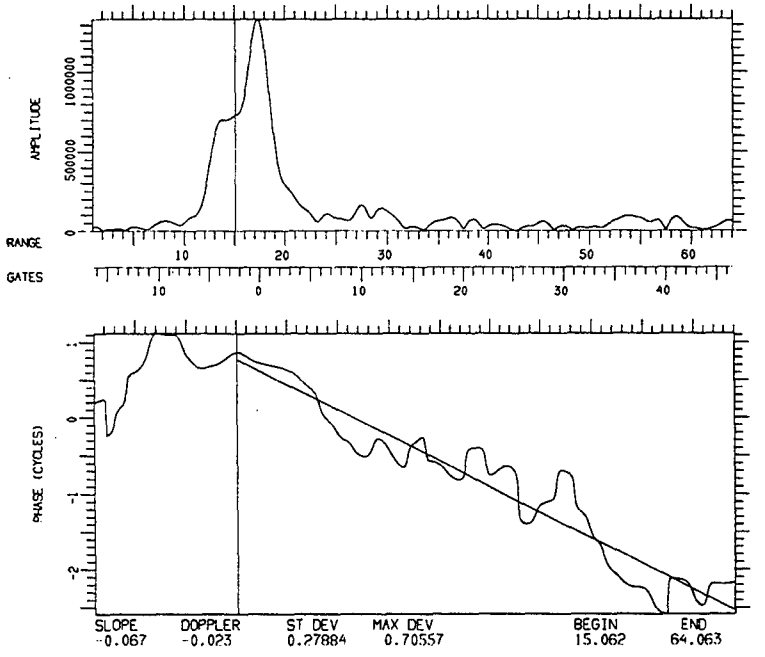

Figure 46. Image Cut in Crossrange Gate 10.02.

Figure 47. There is a well defined phase slope corresponding to Crossrange Gate 17.45. There are other phase slopes in this figure, but they are less well defined and are different from the major phase slope marked in the figure. Use of the TSA thus is problematic.

In this type of measurement there is also an accuracy problem. If we shift the left boundary in Figure 46, the value of the phase slope will change. However, it will change only slowly. Choosing too small of a transform interval by moving the left boundary too much into the response of interest will also give a linear phase slope. Thus we must move the boundary to the left until the phase slope becomes poorly defined. As an example, if the left boundary is moved to Gate 13.5, we obtain the transform in Figure 48. The total deviation of the phase function from linear is now approaching 0.1 cycles, which is becoming significant, and yet the range position differs by less than half a gate, which is 12 cm. The implication is that with an appropriate choice of the boundary the measurement error will be even smaller.

To determine the crossrange position of the scatterer when, as is usually the case in these situations, the response width is much wider than the nominal resolution, we also take the transform, which is shown in Figure 49. The crossrange position again is determined from the phase slope. Although

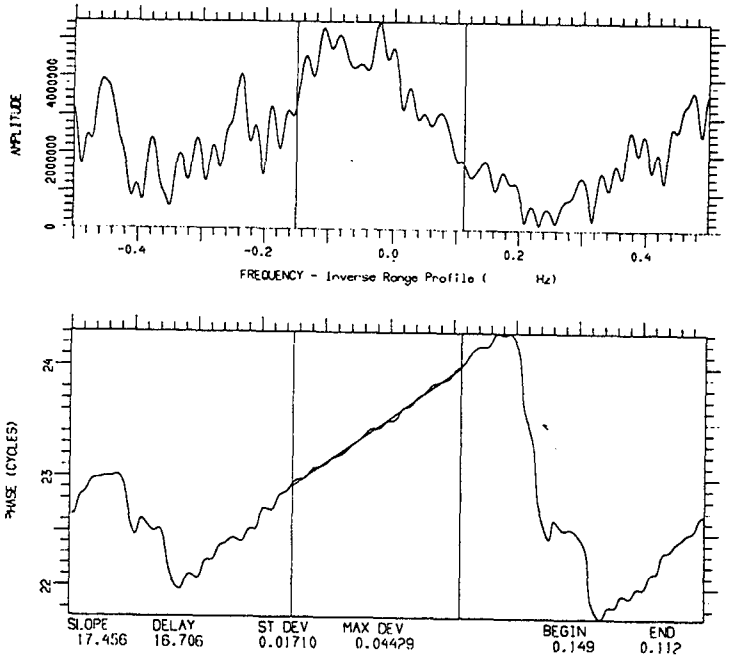

Figure 47. Transform Over Interval Marked in Figure 46.

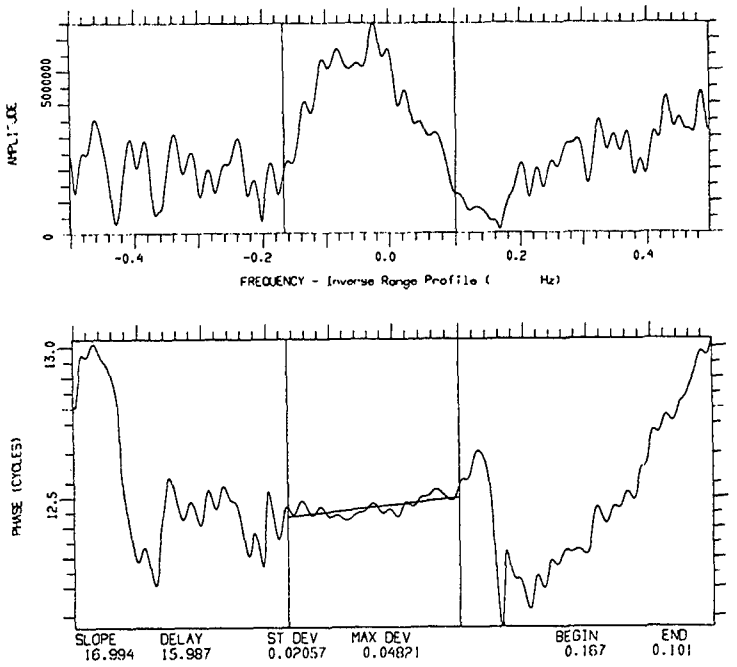

Figure 48. Transform of Figure 46 when Left Boundary is in Gate 13.5.

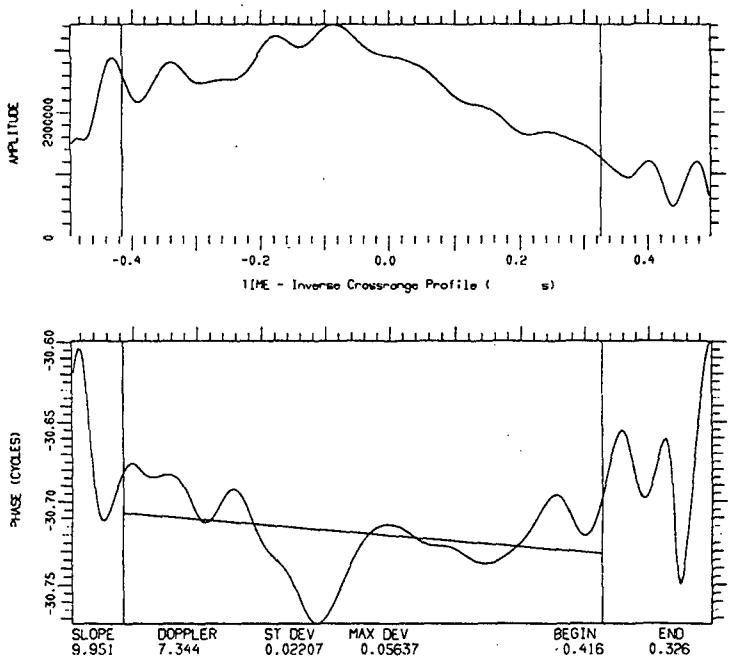

Figure 49. Transform of Image Cut in Range Gate of Response.

the phase appears poorly defined, the scale on the display shows that this is not the case. The maximum phase deviation from the straight line is only about 0.05 cycles.

When the scatterer positions are measured in this manner and then matched to the database used for the TEL on a the straight smooth road, we obtain the positional match in Figure 50. As pointed out, we must allow for a large uncertainty in the measured crossrange positions, because different scatterers will be viewed at different range rates due to the vibrations. Thus, in Figure 50 we must examine how good the match is in range. This match is very good, and it appears to be good enough for identification of the vehicle. We should also point out that the way in which we performed the measurements of the range positions of the scatterers could possibly be improved. This exercise was the first examination of the problem of identifying vehicles with such erratic motion.

The image in Figure 35, which was obtained after a smooth motion compensation in range and Doppler, has an obviously poor quality and yet it resulted in the positional match in Figure 50. Among the data files covering the TEL on a bumpy road we found an even worse set, all of such poor quality that it was difficult to determine which was the worst. One of these images is shown in Figure 51. We will now demonstrate that it is possible to obtain a good positional match even when the TEL is moving so poorly, provided we introduce yet another consideration.

With the image in Figure 35 we were searching the range gates for the time periods over which individual scatterers became dominant, and then performed positional measurements on these scatterers. This approach ignores the possibility that the vibrations could be so large that the resulting measurement errors in range might upset the positional match. In other words, if we compensate the gross motion of the vehicle and choose a long observation period in order to catch all important scatterers in states of constant range rate, the individual scatterers could be displaced in range by a good part of a range cell or even by more than a range cell. Such a long vehicle (13 m) going over ruts, dips, and bumps could easily have some of its parts move independently by a foot or more.

In fact, when we tried the approach used with the image in Figure 35 on the new image, we could not achieve satisfactory positional matches. We had to introduce two changes. First, we reduced the overall observation interval, so as to prevent individual scatterers from moving too much over the interval. Second, in order to accommodate the larger motion compensation residual, we had to develop a new algorithm. The basic TSA applies for a stationary vehicle or one with a perfect motion compensation. To accommodate scatterers

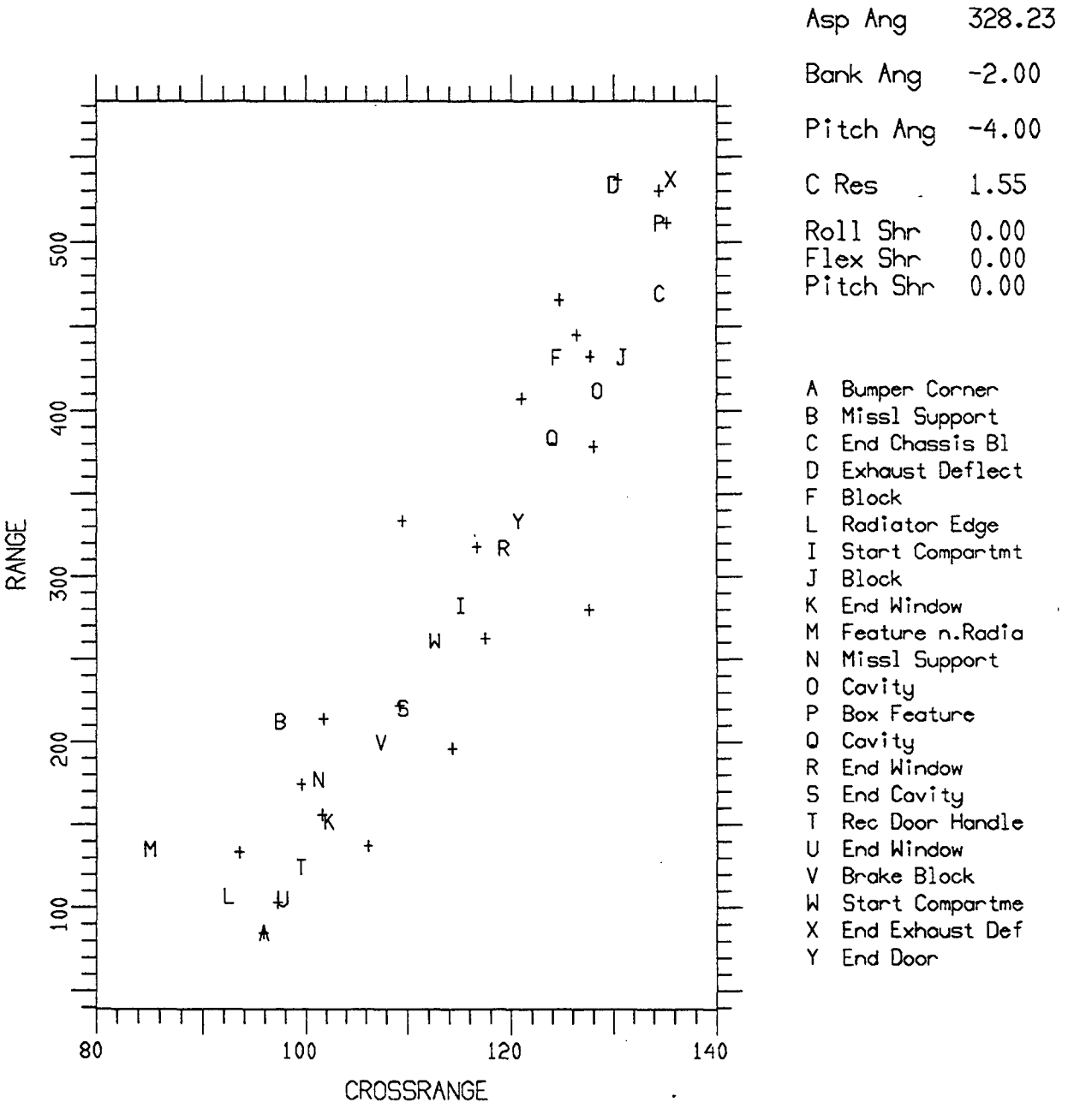

Figure 50. Positional Match of TEL on the Bumpy Road.

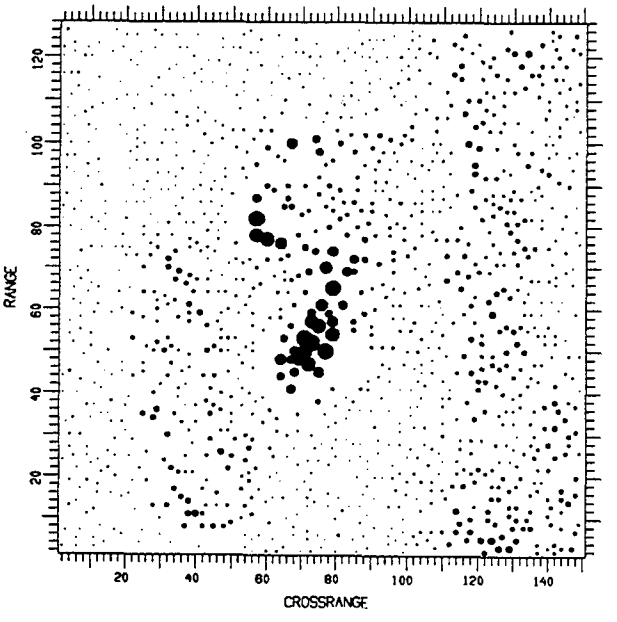

Figure 51. One of the Worst Images of the TEL on a Bumpy Road.

with shifting phase centers whose individual responses would falsely indicate two scatterers if the TSA were used, we introduced a rule that determines when the peak position of a response would be used even when the TSA appears to indicate two scatterers. For such a severe motion as represented by the image in Figure 51, it was necessary to introduce another rule: if the TSA gives a pattern indicative of two scatterers, but this pattern quickly changes to one of a single scatterer when the boundary of the transform window is shifted into the response of interest, we again use the peak position. The TSA pattern then appears only because of the distortions caused by the vibration. These two modifications allow us to obtain a good positional match for these worst-case TEL data.

As a first step, we perform the test in the range gates described earlier, where for those range gates with good scatterers we determine their periods of dominance. The intent of this first step is to shorten the observation period, but we would like to find the best fraction of the original observation time. This means a shorter time interval over which we find the longest periods of dominance. It is equivalent to reducing the original interval of 2 s to the interval with the best vibration behavior of the scatterers. From the examination of the range gates with strong scatterers we

found this interval to extend from -0.1 to 0.4 s on the normalized time scale. The corresponding image is shown in Figure 52. The improvement in the image quality can be seen from the fact that the crossrange spread of the strong responses is far smaller in Figure 52 than in Figure 51. This is so not only because we shortened the imaging time, but also because we selected the best part of the original imaging interval.

With the image in Figure 52 we now must proceed as explained earlier. We want to examine the range gates with strong scatterers, to find their periods of dominance, and to generate subimages over these periods of dominance. For different range intervals or even range gates we then use different subimages. It turned out that with the selection of the best interval in Figure 52, an appropriately chosen time interval essentially overlaps all periods of dominance in the various range gates. Thus we can generate a single image for the positional match, with the new time interval extending from -0.3 to 0.2 s of the normalized time for the image in Figure 52. The corresponding image, for which the imaging interval has been reduced from 2 s to 0.5 s is shown in Figure 53.

We already stated that we had to introduce a new algorithm to determine when there is such heavy vibration to invalidate the TSA measurements. We also explained earlier that in all such cases we must rely on the measurement accuracy in range, using crossrange resolution in order to improve the range measurement accuracy, rather than to achieve good crossrange accuracy. With the same principle, we can also deal with the responses that are offset by the vibration to such a large degree as illustrated by those between Range Gates 80 and 85. We might as well shift these responses in crossrange to roughly the position along the line representing the orientation of the vehicle.

Following the principles explained above, we measured the positions of the scatterers in the image in Figure 53, and then performed the positional match using the same predicted scatterers positions as for the TEL on the straight smooth road. The resulting positional match is shown in Figure 54. We also added uncertainty ellipses at the measured positions, assuming a range uncertainty of only 0.2 gates but a crossrange uncertainty of two gates, as well as uncertainty ellipses at the predicted scatterer positions, arbitrarily assuming an error of 20 cm in position and 5° in angle.

In Figure 54, a good match for a scatterer is obtained if the uncertainty ellipses for the measured and predicted scatterer positions overlap, and in this sense the overall quality of the match in Figure 54 is good. There are only two measured scatterer positions that are unmatched. Taking into account that scatterers close in crossrange are difficult to resolve under such adverse conditions, Figure 54 shows only one predicted position without a

corresponding measurement. It is our assessment that this match demonstrates a high probability that the TEL could be identified even when it is moving in such a difficult environment.

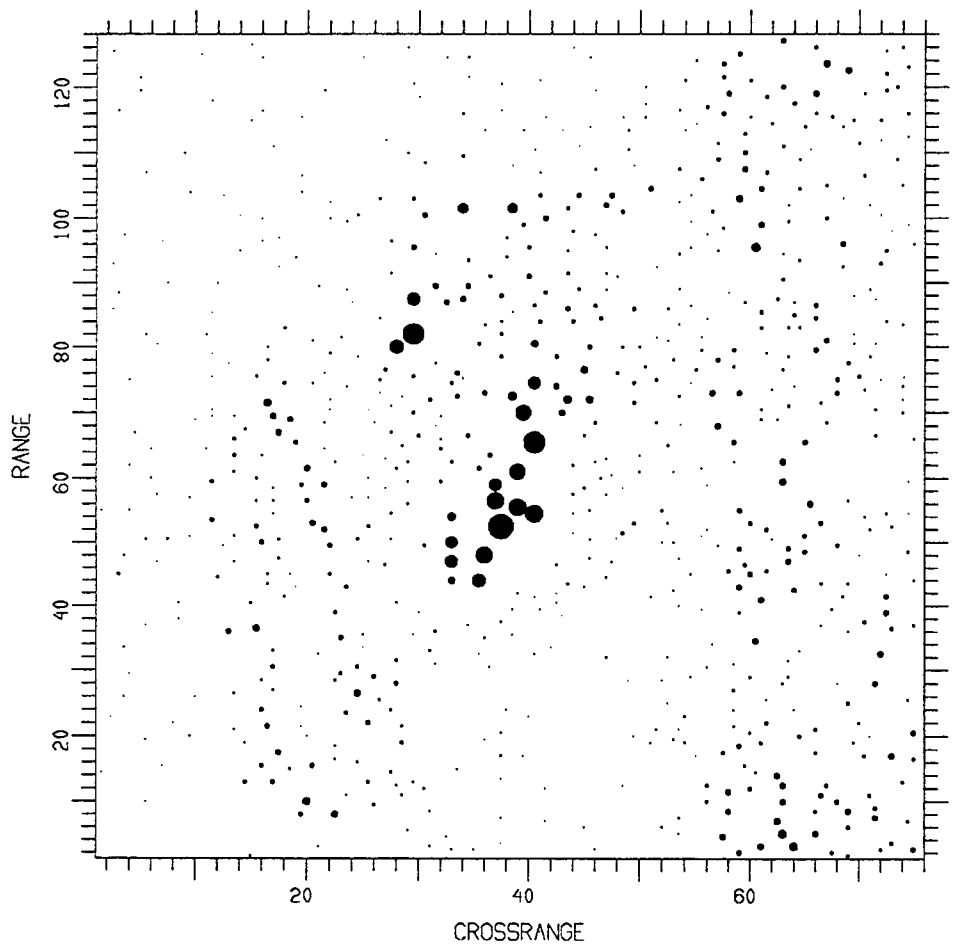

Figure 52. Image Over Time Interval from -0.1 to 0.4 s.

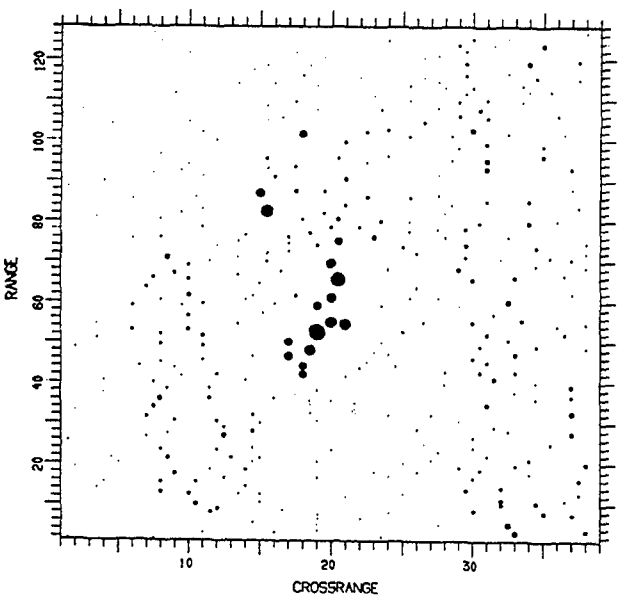

Figure 53. Image to be Used for Positional Match.

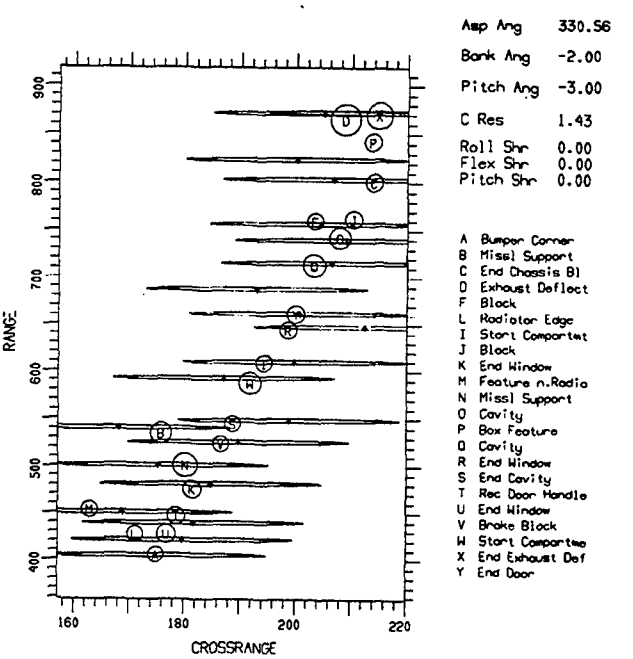

Figure 54. Positional Match for TEL under Worst-Case Motion Conditions.

3. ANALYSIS OF THE M-60 TANK

3.1 The M-60 Moving in a Circle (Data Sets dra010200d019 and dra010200d017)

We will consider extreme cases for the M-60 tank. One such case is almost exactly head-on, so that many of the major scatterers visible for a side view cannot be observed by the radar. On the other hand, the turning and rolling motion of the tank have little impact for this aspect angle, because they do not generate significant range rates or Dopplers. The second case is that of the tank viewed close to broadside. Although the usual scatterers can be observed at this aspect angle, the turning and rolling motions will have strong effects.

3.1.1 The M-60 at Head-on Aspect

As usual with moving ground vehicles, we will observe the vehicle over a longer time than that needed for imaging, in order to select a particularly good interval. This is easy to do with a turning vehicle, because the turning motion provides the aspect angle change needed for crossrange resolution. The peaks plot image of the M-60 generated with a 2 s observation interval is shown in Figure 55. Because of the ineffectiveness of the turning and rolling motions the image is relatively little smeared. Nevertheless, it is still too smeared to permit good positional measurements.

We examine the range gates with major scatterers, take the transforms of the image cuts in these range gates, and then determine the time interval within which each scatterer is strong. An interval which is common to all examined range gates extends from 0.15 to 0.30 s of normalized time. The actual imaging time thus is 0.30 s. The corresponding image is shown in Figure 56. This image evidently is of much higher quality than the one taken over 2 s in Figure 55. Also, from the shadowing we conclude that the vehicle must have a turret. Since the gun muzzle is clearly visible at this aspect angle, we will make use of it to conclude that the vehicle also has a gun. However, most of the time the gun will not be observable in the background. Also, if it is pointed in a different direction, its response may not be sufficiently conspicuous.

We perform the usual measurements in the image in Figure 56, extracting the scatterer positions. For a head-on aspect we will not see the wheels, but we will see the various metallic boxes at the side of the deck. The corresponding positional match is given in Figure 57. The match is very good, except for two unmatched responses. As can be verified from Figure 56, they are weak responses. We do not know what they are, but then one cannot expect

perfect results. The quality of the match in Figure 57 appears sufficient for reliable identification of the vehicle.

We stated above that for a turning vehicle viewed head-on the selection of an optimum imaging time should not be very important. For a test, we selected a sub-interval which, unlike the one chosen for Figure 56, was not good for all range gates. This sub-interval extends from -0.18 to -0.03 s. The image for this interval is shown in Figure 58. At first glance, the image appears to be much inferior to the one in Figure 56, but if the range gates of the major responses are compared with those in Figure 56, we concludes that the image quality is not that much inferior. Although we have not done the positional match for this image, we have little doubt that it also would be successful, even though perhaps not as good as that in Figure 57.

3.1.2 The M-60 Viewed at a Larger Aspect Angle

In the previous section we considered the tank moving in a circle, but with an aspect angle almost exactly head-on. This is a favorable aspect angle because rolling motions and vibrations will not generate strong Dopplers. Now we examine the same tank moving in a circle, but at an aspect angle of about 30°. We will see that the small change in the aspect angle has severe consequences.

The 2-second peaks plot image of the vehicle is shown in Figure 59, with a use of a rather high clipping level in order to enhance the basic features of the image. Only a smooth motion compensation that cannot follow details of the vehicle motion was used. We observe sets of responses repeated in crossrange, the effect one obtains if a near-periodic modulation is superposed on a carrier. This is a consequence of the roll motion of the tank. The roll frequency is so high that the repeated responses fall outside the smeared main responses. This is fortunate because the repeated responses can effectively be ignored. However, it is conceivable that a larger degree of smearing of the main responses could combine with a smaller separation of the repeated responses, so that repeated responses might fall within the smeared main responses. This would considerably increase the severity of the processing problem.

In Figure 60 we give an expanded version of the image of Figure 59, with the lower clip level set at -40 dB from the highest peak. This image provides a better appreciation of the degree of crossrange smearing in the image. In order to extract the scatterer positions from this image, we use the same procedure that was illustrated earlier: we find the range gates with the major scatterers, we take the transforms of the image cuts in these range gates, and we search for the time intervals in which we can observe amplitude

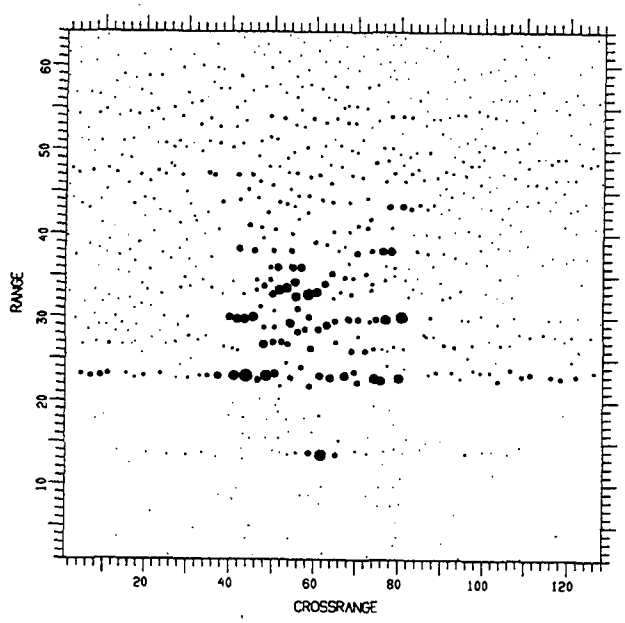

Figure 55. Image of M-60 Head-on.

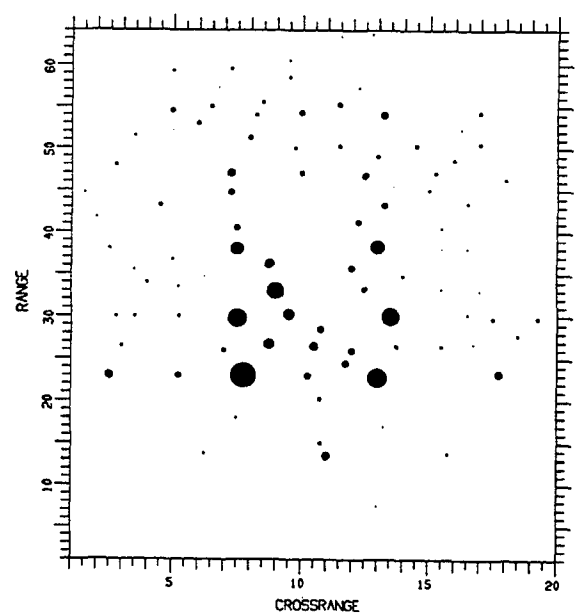

Figure 56. Image of M-60 Over Shorter Imaging Time.

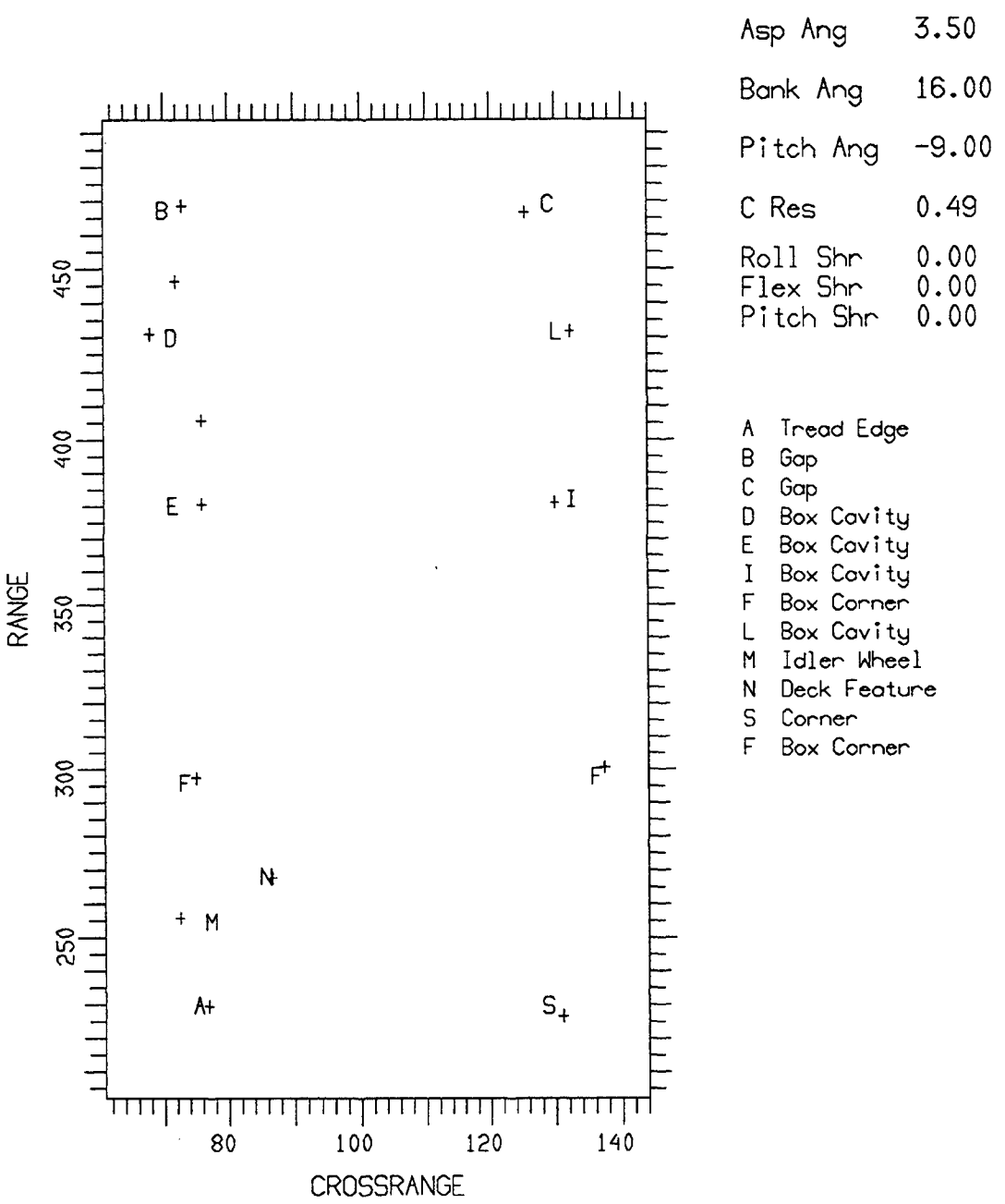

Figure 57. Positional Match for M-60 Head-on.

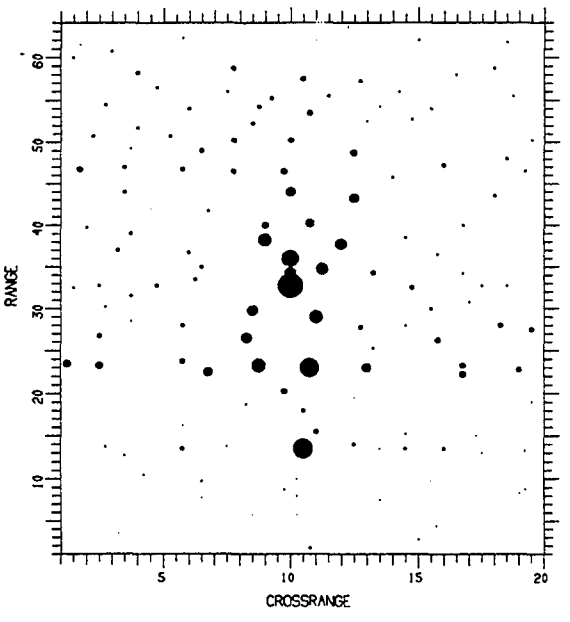

Figure 58. Image for Subinterval from -0.18 to -0.03 s.

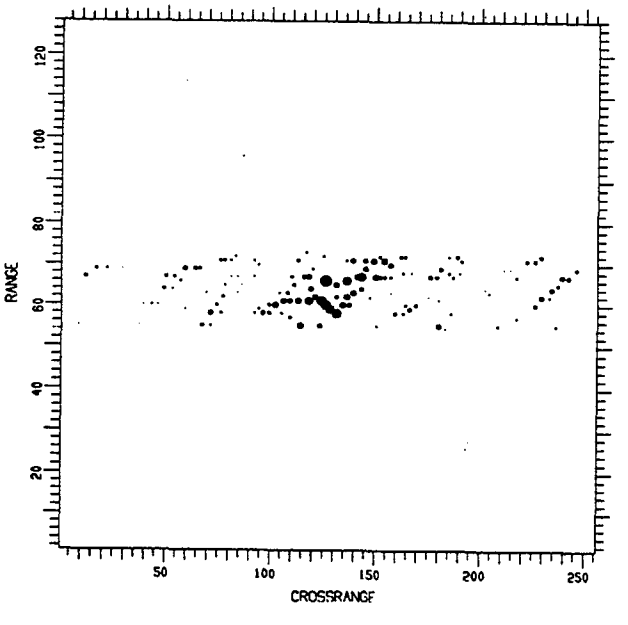

Figure 59. Image of M-60 Moving in a Circle, Aspect Angle of 30°.

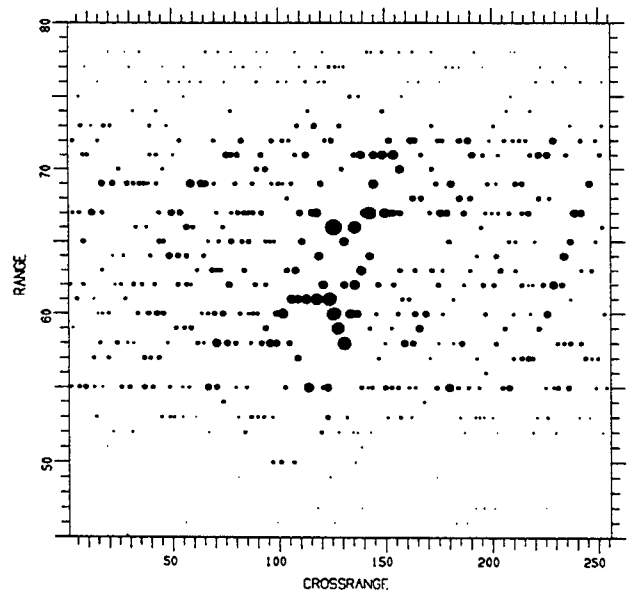

Figure 60. Expanded Version of Figure 59.

peaks of sufficient widths, without deep minima, and associated with phase functions that fluctuate less than about 0.1 cycle about a fitted line. These are the intervals in which scatterer measurements can be performed, via subimages over these intervals.

Because of the arbitrary orientation of the turret, we again largely ignore the responses off the edges of the vehicle. The scatterer positions extracted from the image of the moving tank then are matched to a database of such scatterer positions for a stationary tank at a similar aspect angle. This positional match is shown in Figure 61. To illustrate the relative significance of the match in range and crossrange, in Figure 62 we repeat the match of Figure 61, with the added uncertainty ellipses. We have again assumed (arbitrarily at this point) that the uncertainties of the measured positions are 0.2 gates and 2 gates in range and crossrange, respectively. For the predicted scatterer positions we assumed an uncertainty of 0.2 m in position and 5° in angle. Figure 62 illustrates the fact that we must rely primarily on the range measurements, even though coherent processing over an extended interval is necessary.

There is an interesting point concerning the match of the measured scatterer positions for a moving ground vehicle to the database for a stationary vehicle. Even though a range resolution of about one foot should be adequate for identifying ground vehicles, some of the scatterers may not be

resolved. For example, the M-60 tank has cavities formed by metallic boxes at the edge of the deck, and below these cavities are the cup-shaped wheels. They may be so close in range that they cannot be resolved, or the stronger response might mask the weaker ones. Such effects limit the total number of readily observable scatterers, and the changing phase relations will cause slow changes in the observable scatterers as the aspect angle changes.

When the ground vehicle is moving, in particular when it is moving in an erratic manner, the phase relations between scatterers are rapidly and continuously changing. By examining the data over a longer interval, we then obtain glimpses of a larger variety of scatterers than is possible when the vehicle is stationary. At the expense of more extensive processing, we thus can detect more features when the vehicle is moving. This was found to be true with the image in Figure 60, although we did not try to determine just how many more scatterers one might observe than were observable on the stationary target that served as a database.

3.2 The M-60 on a Straight Road

The experience with the M-60 tank moving in a circle in flat desert terrain suggests that motion on a bumpy road might pose even more difficult problems. However, no data are available on either the M-60 or the M-109 on the smooth or bumpy road.

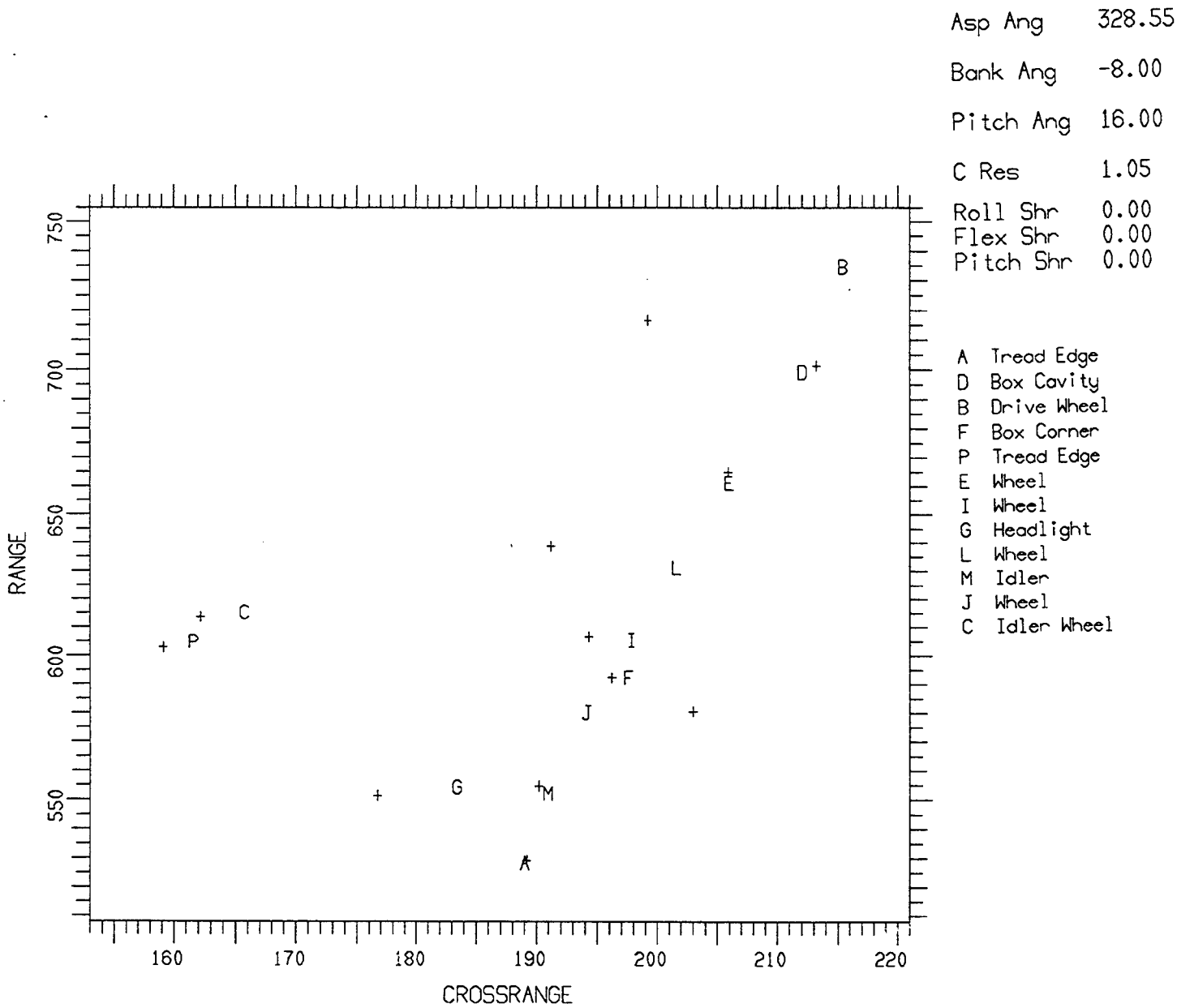

Figure 61. Positional Match of Scatterer Positions from Moving Tank with Database from Stationary Tank.

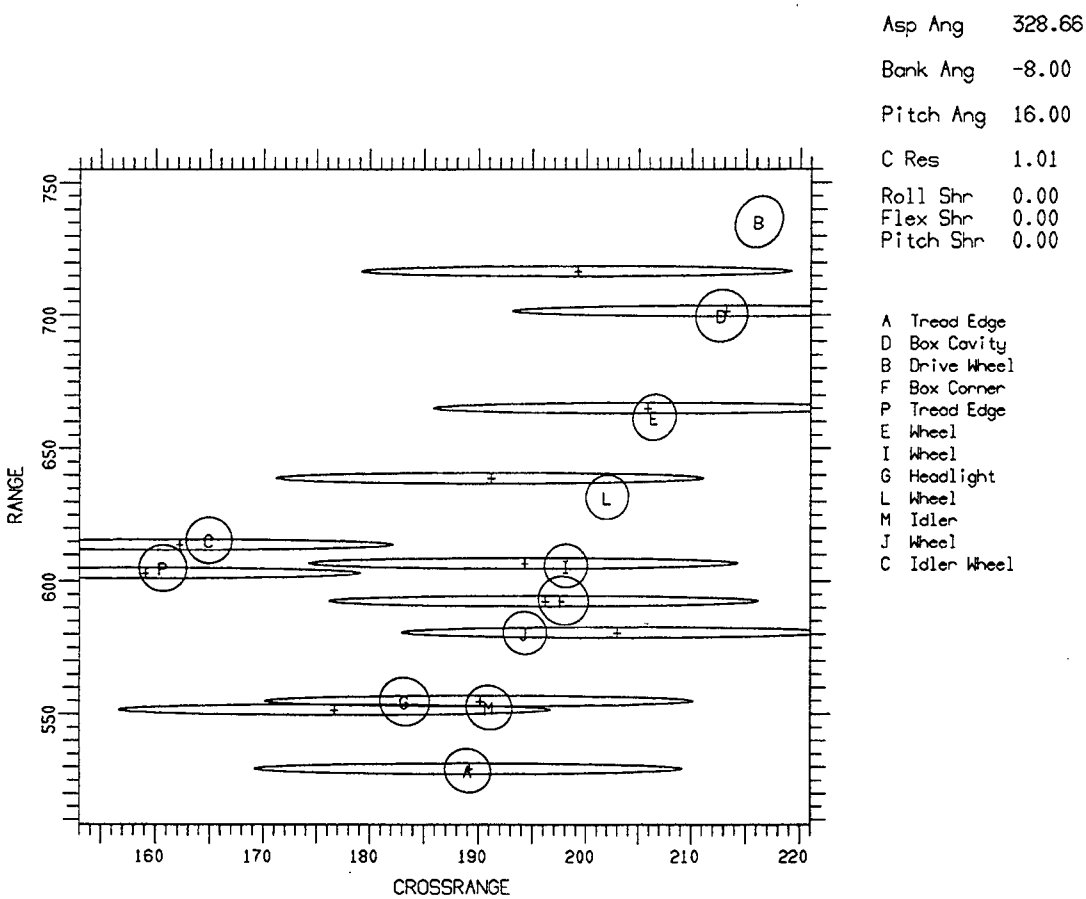

Figure 62. Positional Match with Uncertainty Ellipses.

4. THE M-813 TRUCK ON A BUMPY ROAD (DATA SET dra030500a006)

The extensive analysis of the TEL has shown that among all types of conditions the movement on the bumpy road poses the most challenging identification problems. Since data from treaded vehicles on the bumpy road are not available, we have analyzed the M-813 truck on the bumpy road.

A 2-second image with only a smooth motion compensation is shown in Figure 63. This is one of the worst images we found. However, it is important to analyze images of poor quality, because a surveillance radar cannot choose the time at which it observes a particular ground vehicle. As always, we must analyze one or more range gates in order to understand the situation and choose the appropriate approach.

In Figure 64 we show the transform of the image cut in Range Gate 77.05, which is perhaps the cleanest of the range gates. Since the amplitude does not show any deep minima, the range gate is dominated by a single scatterer, and the phase function describes the motion of this scatterer. The amplitude and phase functions tell us that the vehicle motion is much worse over the first half of the observation time than over the second half. In practice, we would choose the second half for analysis. Since our present interest is research, we will attempt to analyze the truck under the worse motion conditions of the first half.

In contrast to the second half of the observation time, the first half shows a rather large cyclical motion of the scatterer. The phase deviation is about three cycles, so that the scatterer moves back and forth by about 1.5 wavelengths or nearly 5 cm. We could compensate this motion and generate a good image of the scatterer. However, the scatterers on other parts of the vehicle move differently, so that they would all have to be compensated individually. Even then, their different motions could displace them far from the actual crossrange positions of the scatterers. The implication is that ultimately we will have to rely on range measurements for the identification.

As can be seen from the linear trend of the amplitude in Figure 64, the scatterer is drifting in its range cell. This trend is disturbed by two amplitude spikes, which coincide with a reversal of the direction of motion. This is not the first time we observed such an effect, but it cannot be explained on the basis of the motion within the range cell, as can the linear trend. We believe the effect to be be caused by the basic backscattering mechanism of such scatterers. The subimages over the two halves of the imaging time in Figure 64 are shown in Figures 65 and 66. Evidently, the image in Figure 65 is much worse than the one in Figure 66. We will analyze the worse of these images.

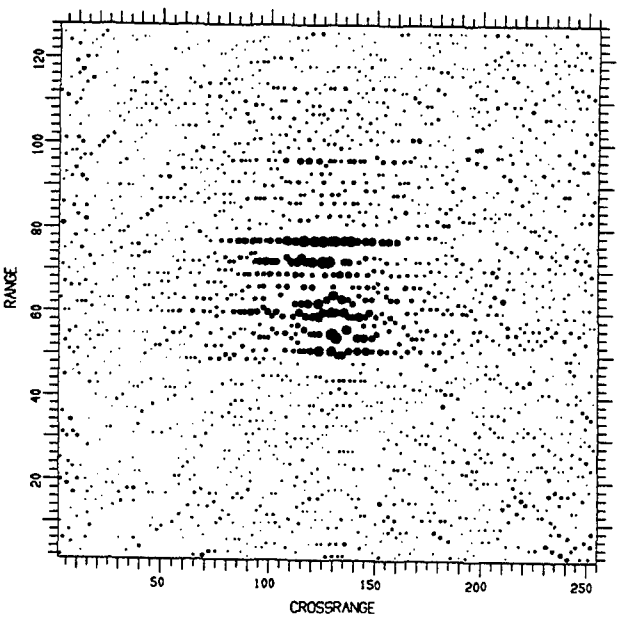

Figure 63. Image of Truck on a Bumpy Road.

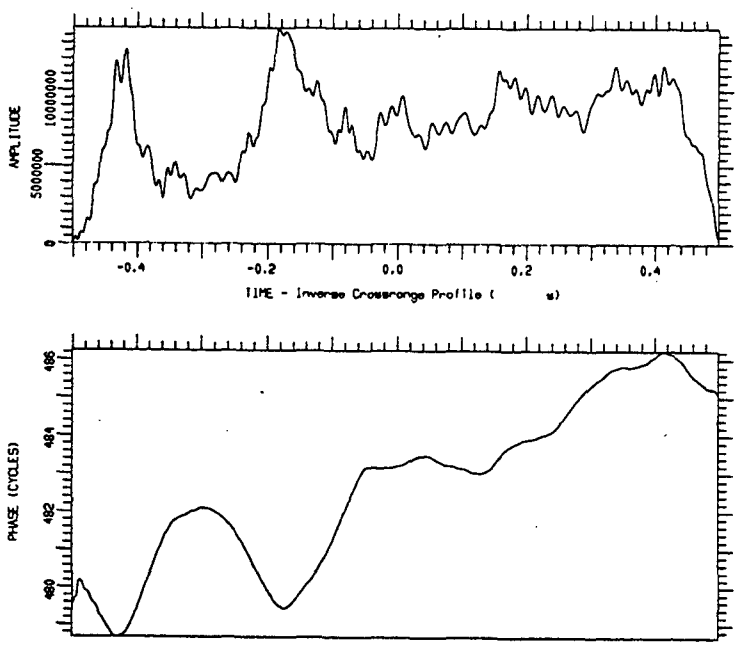

Figure 64. Transform of Image Cut in Range Gate 77.05.

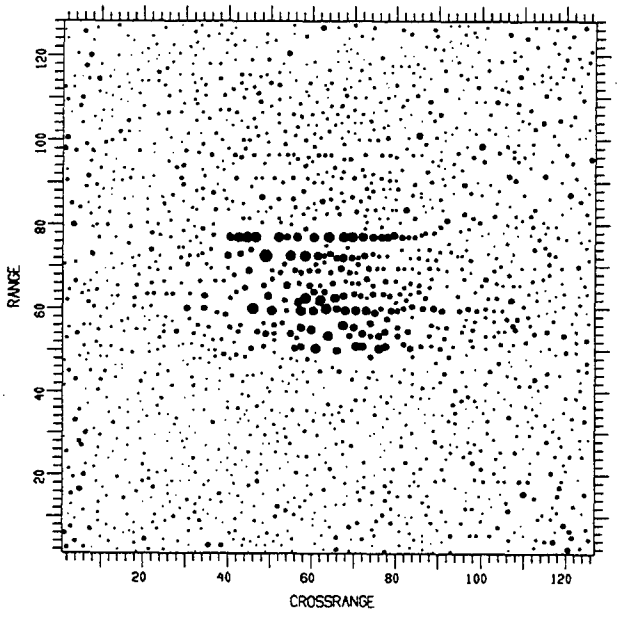

Figure 65. Image Over First Half of Imaging Time in Figure 64.

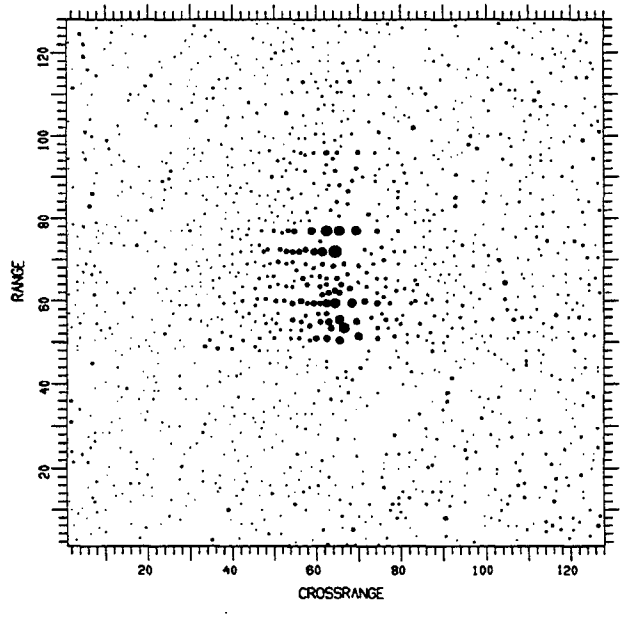

Figure 66. Image Over Second Half of Imaging Time in Figure 64.

The analysis principles developed earlier for the other moving vehicles also apply for the truck on the bumpy road, but the processing is more critical. To explain the situation, in Figure 67 we repeat the first half of the amplitude and phase functions of Figure 64, which are also the amplitude and phase functions of the corresponding image cut in Figure 65. The slope of the phase function is Doppler, and our software is normalized such that the phase slope corresponds to the crossrange position in gates. The printout on the right margin shows that the first phase slope corresponds to Crossrange Gate 80.46, and the second to Gate 42.14. The scatterer thus shifts by nearly 40 crossrange gates in a time of about 1/3 second. If we want to measure the crossrange position of the scatterer, what time do we choose? Whatever time we select, since the motions of the individual scatterers are not synchronized, their responses may also be shifted in crossrange. Moreover, other scatterers may not even be observable at the selected time. If we choose another time, an even larger uncertainty in crossrange position is introduced. The conclusion is that we cannot rely on crossrange measurements, and must base the identification on range measurements alone. Nevertheless, a longer observation time and some crossrange processing are evidently still necessary.

We analyzed the range gates that contain significant responses in Figure 65, using the same methods as illustrated earlier in considerable detail. We then matched these measurements to a database of scatterer positions that we derived from the M-813 truck at a similar aspect angle, but when it was stationary. We took the high variability in crossrange position into account by allowing a crossrange uncertainty of 20 gates, whereas the range uncertainty was assumed to be 0.2 gates. For the predicted scatterer positions we again assumed an uncertainty of 0.20 m in position and 5° in angle. The resulting positional match is shown in Figure 68. The quality of the match appears completely satisfactory, despite the extreme motion behavior of the truck and the use of tentative processing and analysis methods.

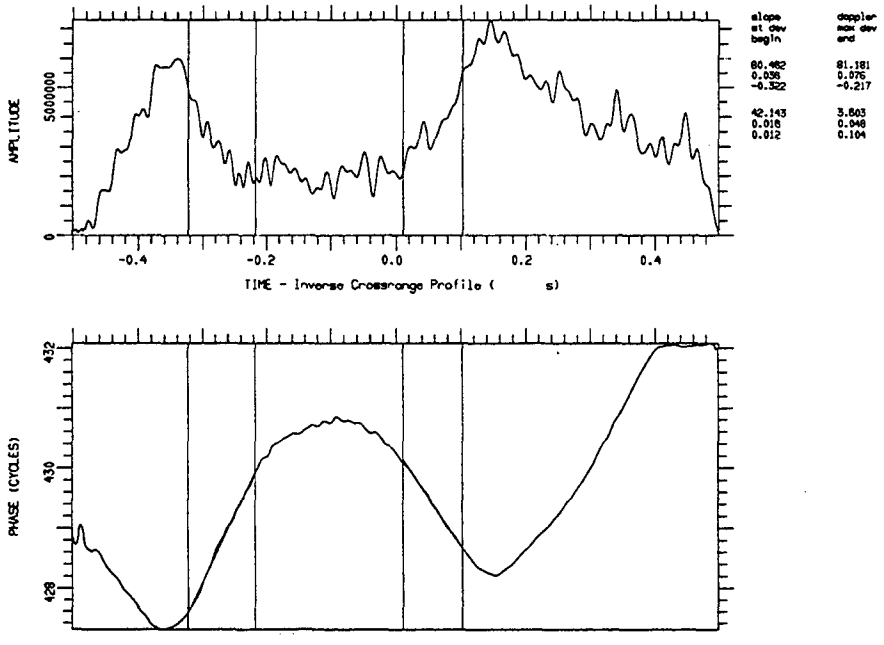

Figure 67. Repeat of First Half of Figure 64.

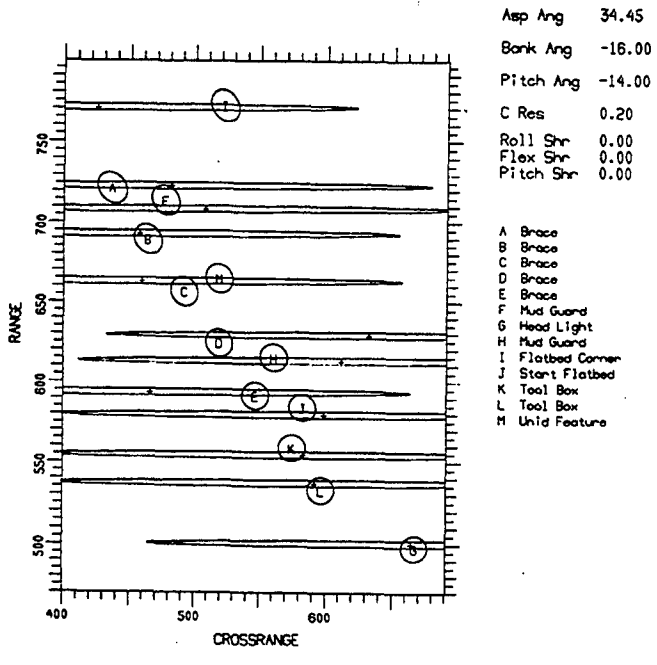

Figure 68. Positional Match for M-813 Truck.

5. SUMMARY

In this section we summarize the situation concerning the identification of moving ground vehicles, and the role of one- and two-dimensional processing (HRR and SAR/ISAR).

Ignoring the ground clutter for the moment, we start with a stationary ground vehicle. Since a ground vehicle is much longer than it is wide, it is simpler to identify the vehicle when it is viewed at a small aspect angle. Range resolution then is very effective in subdividing the vehicle into small parts. With the use of one-dimensional high range resolution (HRR) we obtain a range profile. At a small aspect angle, the major scatterers will provide responses that are fairly well resolved, so that the range positions of the response peaks will often correspond to positions of actual scatterers (which we are attempting to measure). The lower-level peaks will largely represent the peaks of an interference pattern, so that the peak positions are meaningless. If we use additional crossrange resolution, or two-dimensional imaging, the scatterers in each range gate will be largely resolved by crossrange resolution, so that the positions of the response peaks will be more meaningful. This is particularly important when the aspect angle approaches broadside, because then range resolution is less effective and the number of significant scatterers in each range cell increases.

Let the ground vehicle now be moving. An important consequence is that, except for range rates near zero, the ground clutter can be suppressed either by Doppler filtering or by DPCA processing. With low range rates, on the other hand, we have a situation similar to that for stationary targets, which mask the clutter underneath. Thus we need not consider the ground clutter here, in particular since it is insignificant for the Dragnet/MTE environment. However, the motion of the vehicle has important consequences on both range profiles and two-dimensional images.

We consider first the simplest case, a wheeled ground vehicle viewed at small aspect angles. As stated above, some prominent scatterers will give good responses whose peak positions are those of the associated scatterers. However, two detrimental effects appear. First, as the motion of the vehicle causes the aspect angle to change, the phase relation between scatterers will change, and hence the interference will vary between constructive and destructive. Sometimes a particular scatterer will be readily visible, and at other times it will not. Second, the prominent scatterers are the type that tend to trap the radar wave, such as cavities and cavity-like features. The aspect angle change due to the vehicle motion will cause the phase center of such a scatterer to shift, so that the corresponding phase changes add to

those caused by the aspect angle change with a stable phase center. This implies that the interference effects are stronger and occur faster. The positions of the peaks in the range profile will less frequently be those of the actual scatterers. Also, more and more widely spread spurious responses are generated.

We will give an illustration based on the image in Figure 32, which is the TEL moving on a bumpy road. Even though a later section of the data shows more severe effects (Figure 51), they are already bad for Figure 32. In Figure 69 we show the sequence of range profiles used to obtain the image in Figure 32. The aspect angle of the TEL is about 32°. We see two responses that are fairly well trackable. However, most responses are not, because they represent interference patterns rather than the resolved responses from specific scatterers. The same situation persists if we continue the plot of the range profiles. It is evident that one could not extract positional information from the range profiles themselves that is needed to identify the vehicle.

Next we show a set of range profiles from the tank moving in a circle. The aspect angle is close to that of the TEL on the bumpy road. A sample sequence of range profiles is shown in Figure 70. Earlier and later range profile plots all have a similar appearance. The figure clearly illustrates that no response is trackable, except perhaps at the upper part of the figure, but only for a very short time.

We can draw several conclusions from these two sets of range profiles. First, for the same aspect angle, a wheeled vehicle on a bumpy road is still a more benign case than a treaded vehicle moving over flat desert. Second, whereas there is little chance of identifying the wheeled vehicle based on range profiles alone, there is absolutely zero chance for identifying the moving tank. Third, as seen from the earlier examples, for moving ground vehicles we cannot form two-dimensional images of a quality sufficient to extract feature positions. We are stating that range resolution alone will not do, and that the generation of two-dimensional images of the required quality is impossible. This conflict is resolved by using Doppler processing, but in a different way. As illustrated, we utilize Doppler processing primarily for finding those times at which it happens to be possible to utilize range resolution for the measurement of the range positions of the scatterers. We may obtain some additional benefits from Doppler/crossrange resolution, but the primary benefit is to allow an accurate range measurement on the scatterers.

Specifically, for successful identification we must observe the target over a longer period, making a crude image. In this image we examine the

individual range gates and search for those intervals in which one or more responses become visible, because the conditions happen to be right. At these times we can measure the ranges of the associated scatterers. We can also make crossrange measurements, but these will be governed by so many accidental motion conditions that they will often be useless. The situation becomes more difficult as the aspect angle approaches broadside, because range resolution is much less effective. This is predictable. On the other hand, we have also found that the jerky motions of treaded vehicles present a much bigger problem than the smoother motions of wheeled vehicles, even on a bumpy road.

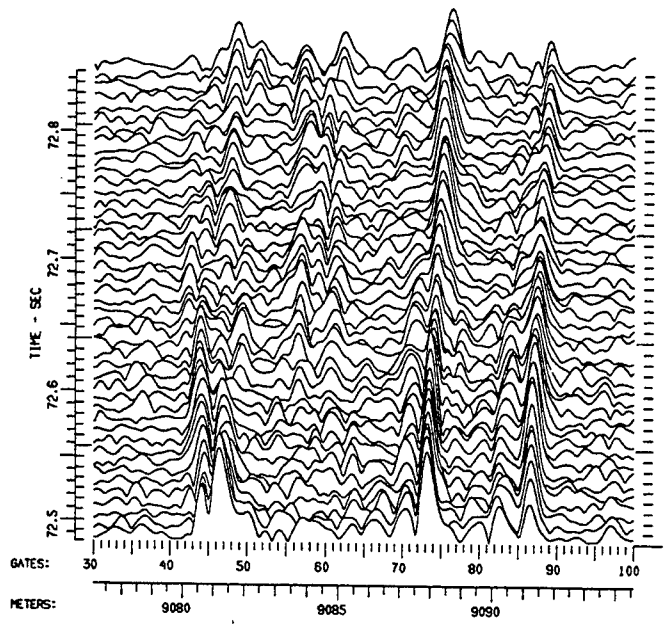

Figure 69. Range Profiles for TEL in Figure 32.

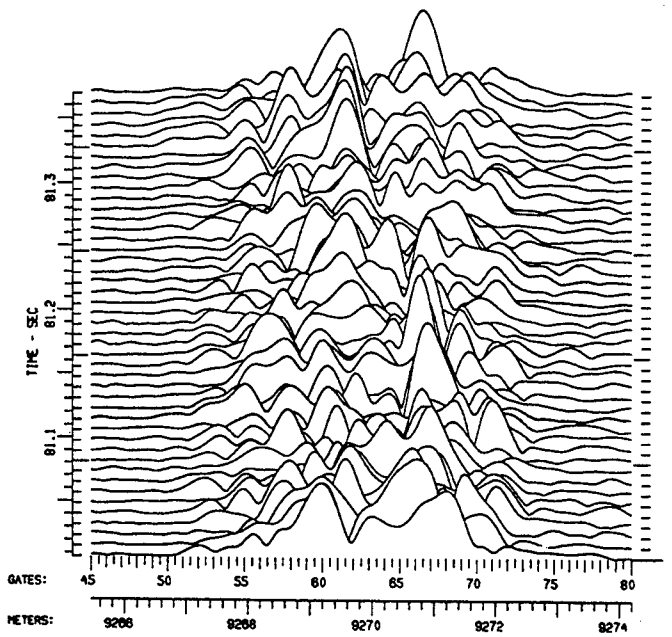

Figure 70. Range Profiles for Tank Moving in a Circle.

6. CONCLUSIONS AND RECOMMENDATIONS

It is our longstanding belief that reliable identification of stationary ground vehicles cannot be based on the intensity image, by attempting to interpret this image as if it were a crude photograph. We conclude from the above work that any attempt at this type of identification for moving ground vehicles makes even less practical sense. Identification of moving ground vehicles in SAR imagery thus cannot be performed by generating nice looking images and somehow interpreting these images. Instead, we must form a crude image by removing only the gross motion of the vehicle, and then extract from this image those measurements on which identification can be based. The most important measurements are those of the positions of the major scatterers on the vehicle. When the motion is relatively benign, it can be the range and crossrange positions; but with increasing motion complexity only the range measurements remain usable.

It has also become evident that the details of the analysis procedure are variable, depending on the type of vehicle (wheeled or treaded) and the severity of its motion. The implication is that the processing must be adaptive. A crude image is formed, using the standard motion compensation procedure. Then we analyze several image cuts with major and reasonably well resolved scatterers. Depending on the results of this analysis, we adopt a specific analysis approach. The results of this program are a clear indication that reliable identification of moving ground vehicles should be possible.

To develop a practical identification method, the following steps are recommended for a follow-on program:

1. The processing and analysis procedures described in this report should be analyzed further, so as to arrive at a set of well formulated processing algorithms that apply for all vehicles under all motion conditions.
2. These algorithms should be fully automated and tested on the entire range of Dragnet/MTE data, and then adjusted until they give the required measurement performance.
3. The possibility of utilizing additional information for vehicle identification should be investigated, perhaps to augment the performance obtainable from the positional match.
4. The actual identification procedures should be implemented, based on our experience in this field.

5. One should demonstrate that all vehicles in the Dragnet/MTE data set can be reliably identified under all conditions of motion.